Novel Interconnect Characterization Techniques

Scott List
Intel Assignee at IMEC
Kapeldreef 75
Leuven, Belgium 3001

Characterization Outline

- General Scaling Challenges for Metrology
- Interconnect Grand Challenges
    - Interfaces
    - Structure
    - Mechanical Properties
- Conclusions
- References

Goals:

- Define interconnect characterization challenges
- Introduce fundamental physics and examples of novel characterization techniques
- Identify remaining metrology gaps
- Provide opportunities for interactions and potential future collaborations

Metrology Scaling Challenges

- Metrology spot sizes don’t scale with Moore’s Law

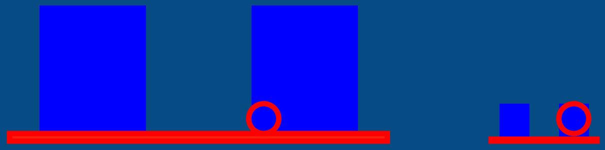

- Need intrinsic 3D information

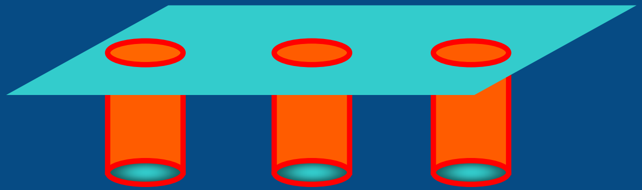

- Characterization of thin, buried layers

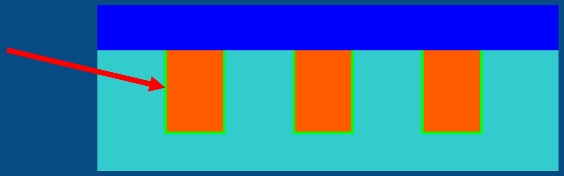

- Interfaces are becoming more dominant

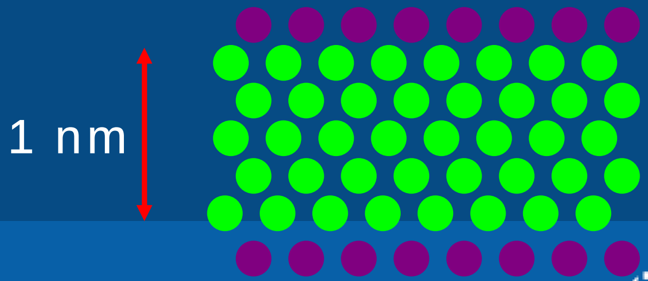

Interconnect Grand Challenges

- **Interfaces**
  - Sidewall damage/etch residues
  - Thin barriers
  - Sidewall scattering

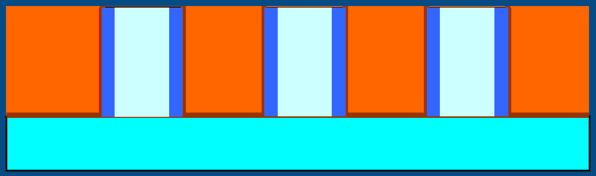

- **Low k & Cu Structure**
  - Porosity and Sealing
  - Bonding Structure
  - Barrier and Cu texture/grain size

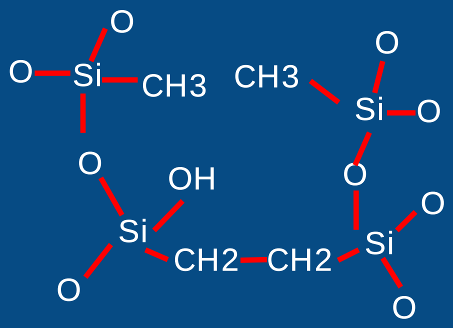

- **Mechanical Properties**
  - Young’s modulus, hardness
  - Adhesion
  - Fracture Dynamics

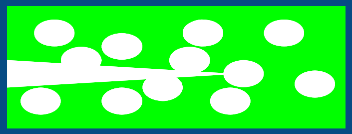

Interface Characterization

- **Interfaces**
  - Sidewall damage/etch residues
  - Thin barriers
  - Sidewall scattering

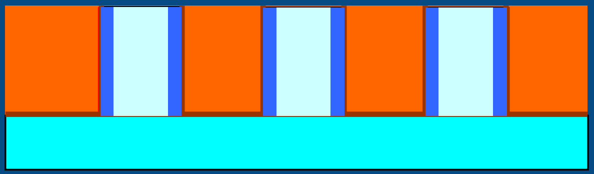

Novel Characterization Techniques

X-ray Reflectometry
Electrostatic Force Microscopy
Atom Probe
TEM Tomography
Electron Spin Resonance

X-ray Reflectometry (Physics I)

XRR involves monitoring the intensity of the x-ray beam reflected by a sample at grazing angles.

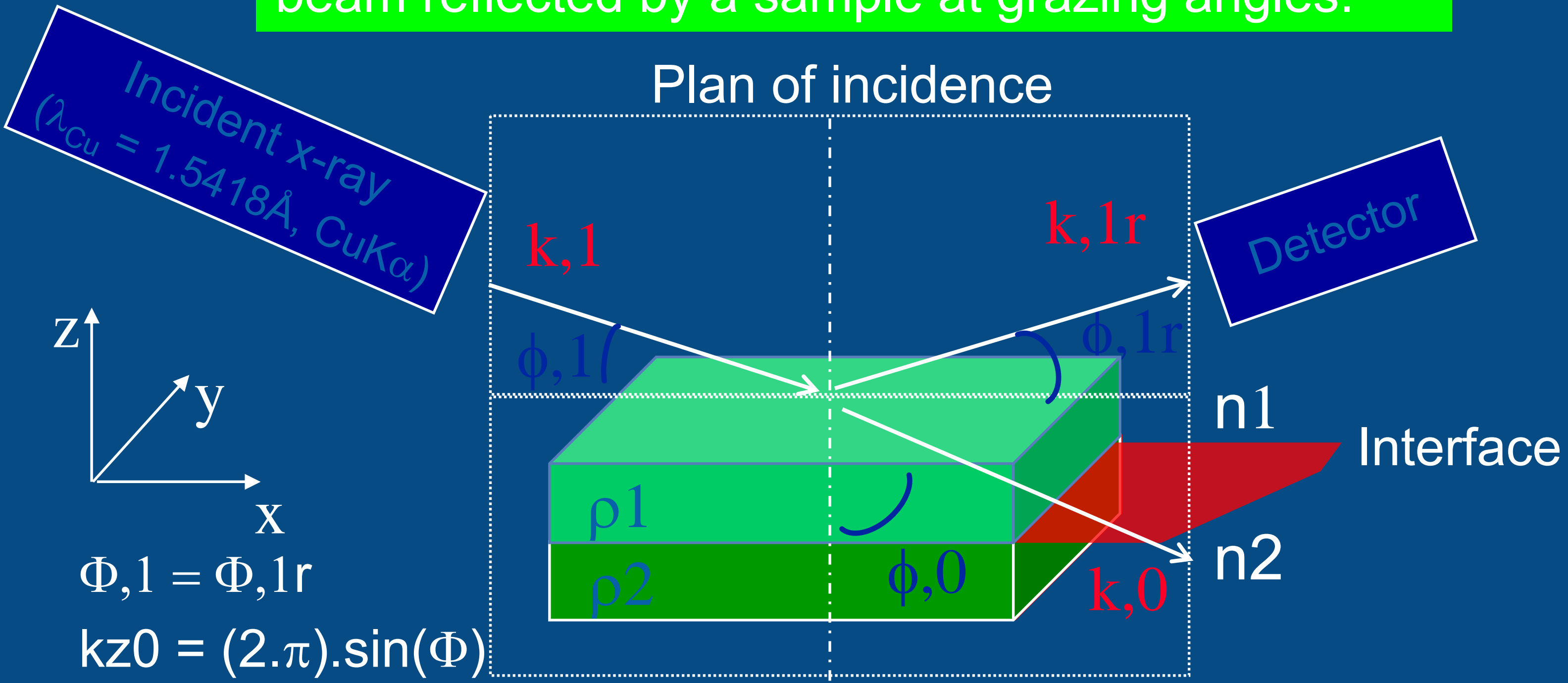

$$\Phi,1 = \Phi,1r$$

$$kz0 = (2.\pi).\sin(\Phi)$$

Refractive index of matter for x-rays of wavelength λ:

$$n(z) = 1 - \rho\frac{\lambda^2 r_0}{2\pi} + i\frac{\lambda}{4\pi}.\frac{1}{\mu}$$

Reflectivity from real surface:

$$R(kz) \propto \int \left\langle \frac{d\rho}{dz} \right\rangle e^{2ikz}\, dz$$

X-ray Reflectometry (Physics II)

[1] Travaly

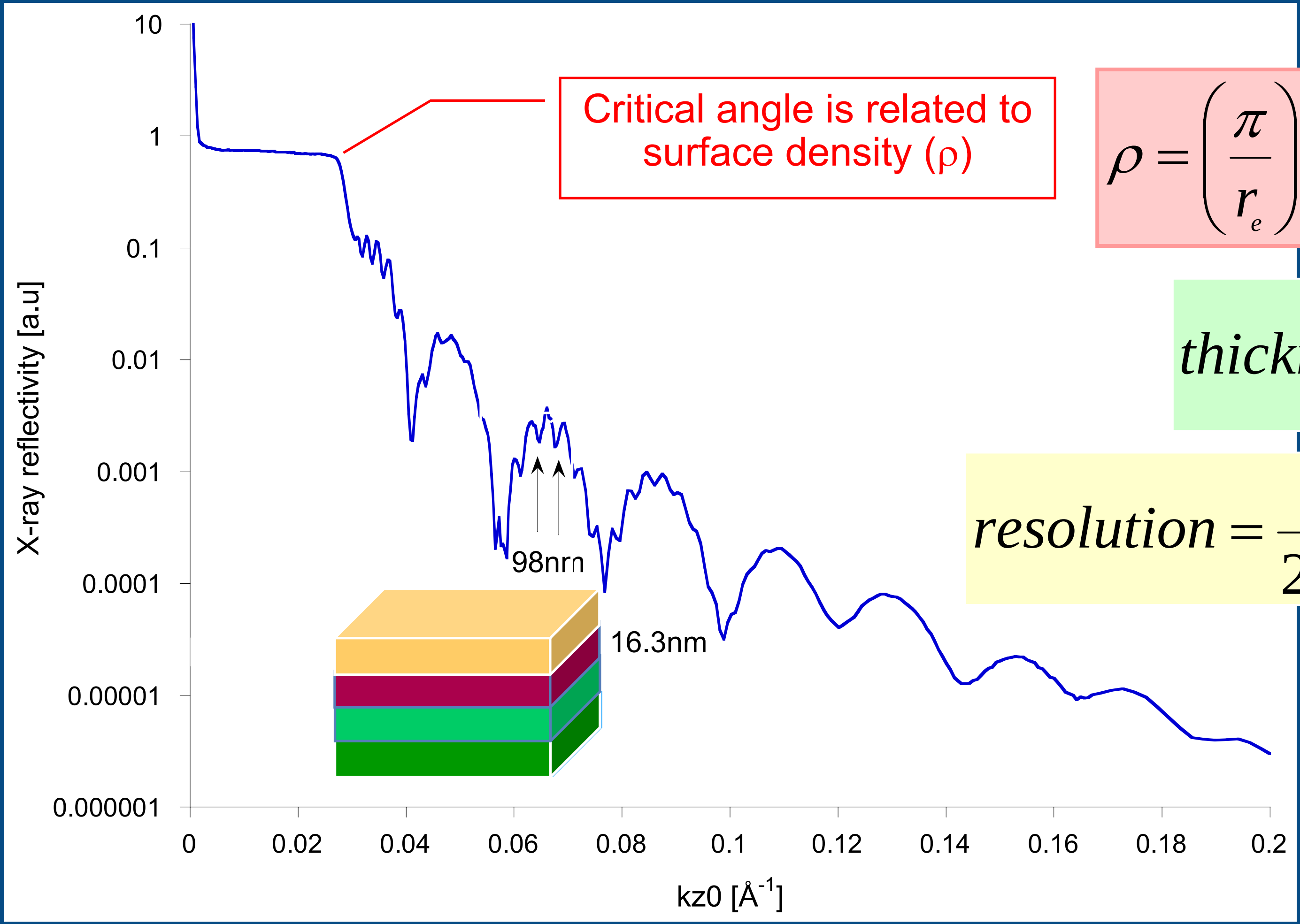

Critical angle is related to surface density (ρ)

$$\rho = \left(\frac{\pi}{r_e}\right)\cdot\frac{\theta_c^2}{\lambda^2}$$

$$thickness = \frac{\pi}{\Delta kz0}$$

$$resolution = \frac{\pi}{2*0.35} \approx 5\text{Å}$$

At least 2 periods are visible, presence of a multi-layer stack

X-ray Reflectometry (Example)

[1] Travaly

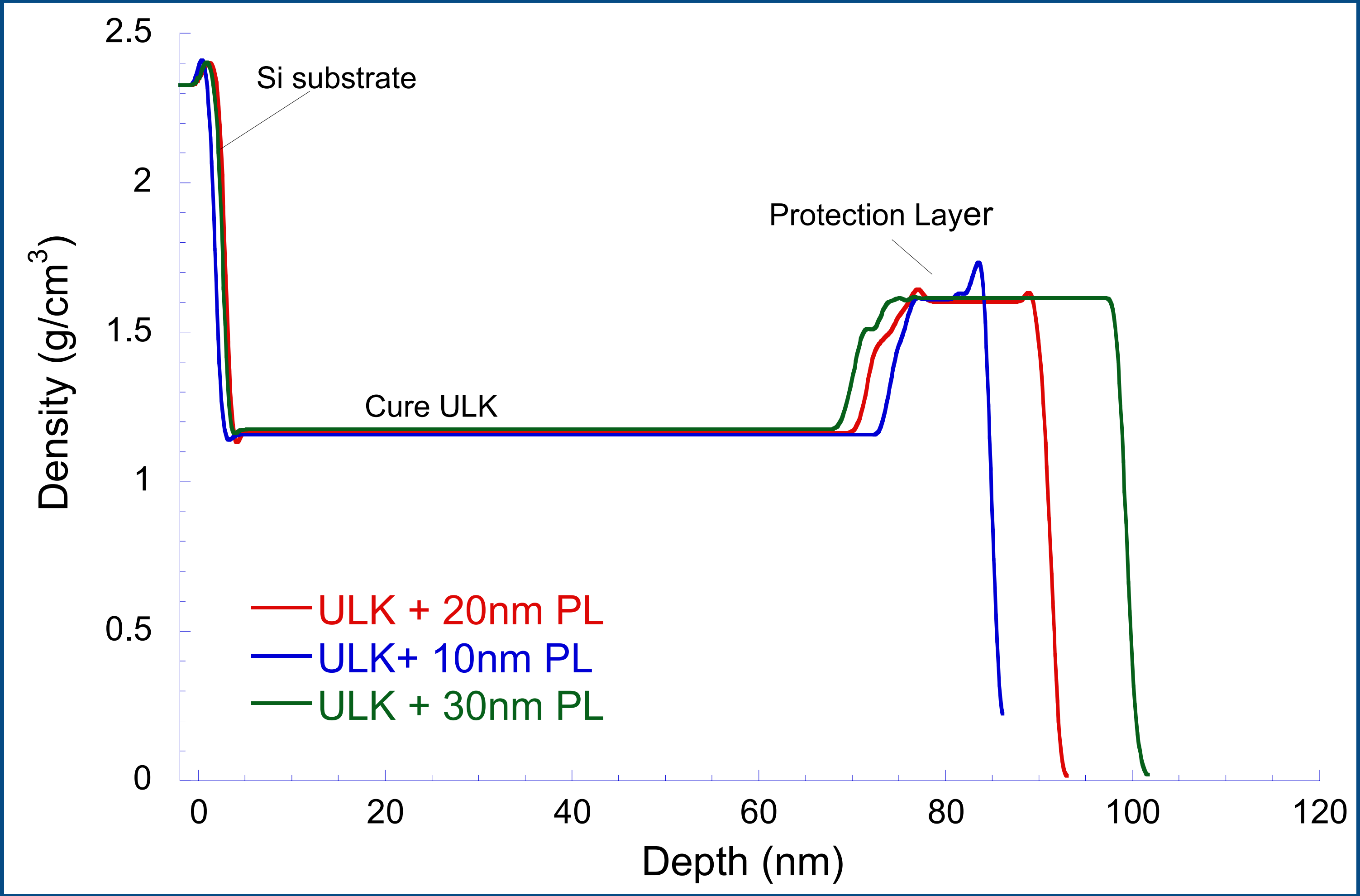

Electrostatic Force Microscopy (Physics)

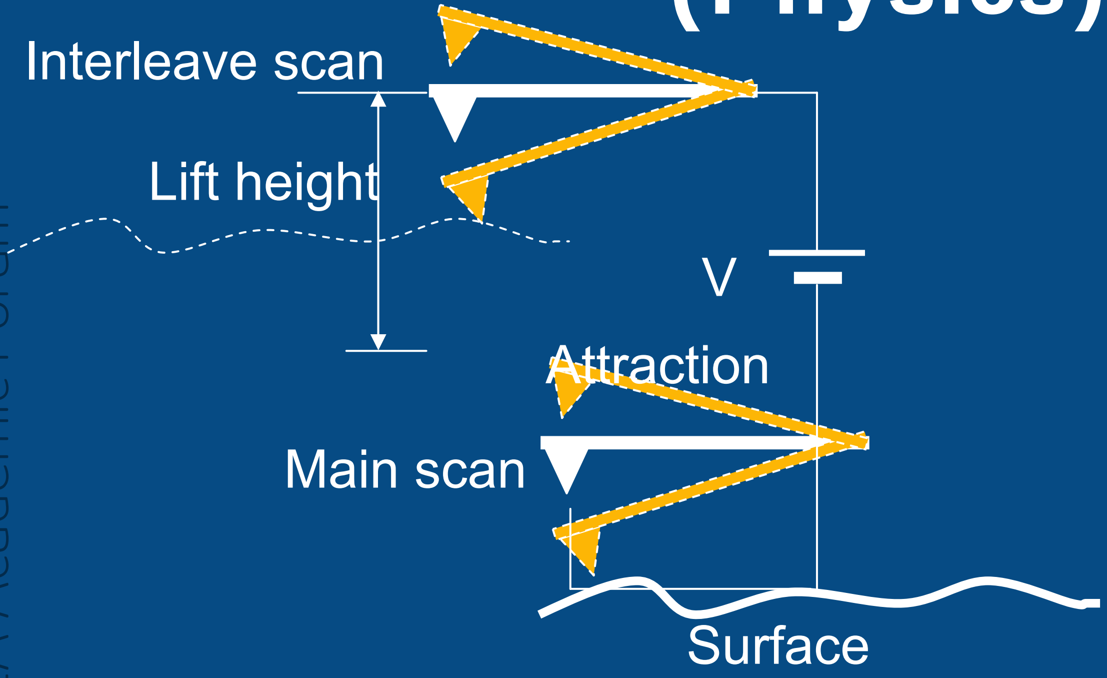

Main scan → Topography

Interleave scan → Phase image or frequency image

Attraction

Resonance frequency shift

Electrostatic Force Microscopy (Physics)

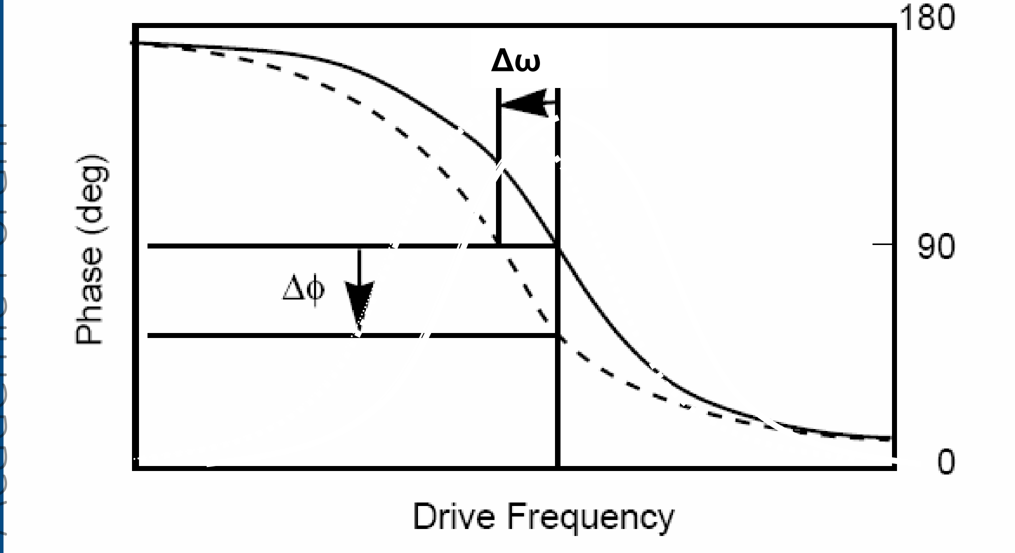

$$\Delta\omega \cong \frac{\omega_0}{2k_0}\frac{\partial F}{\partial z}$$

k_o is cantilever spring constant

ΔΦ – Phase shift
Δω -Resonance frequency shift

Force gradient (which is proportional to the dielectric constant) is proportional to the resonance frequency shift or phase shift.

Electrostatic Force Microscopy (Example)

[2] Gross

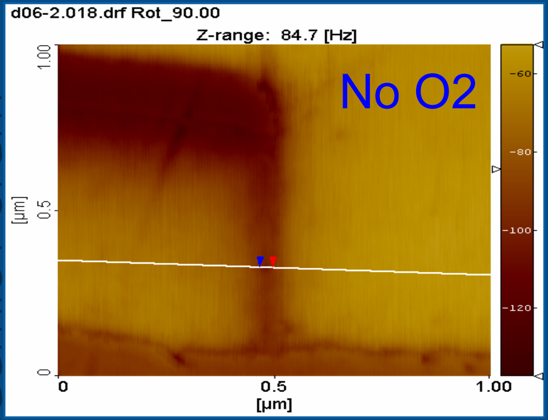

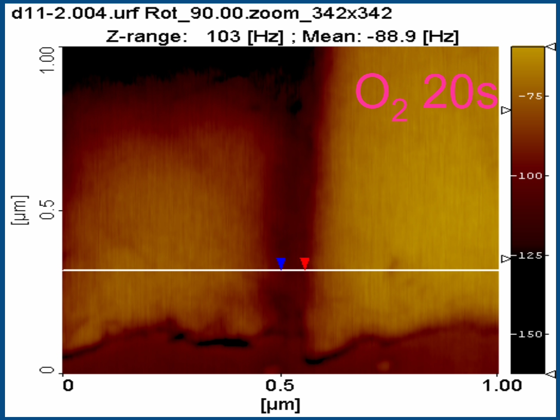

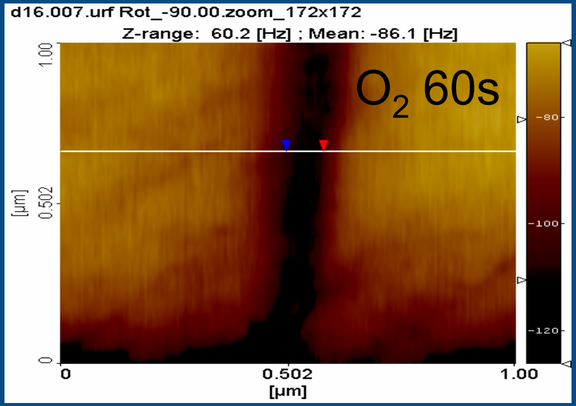

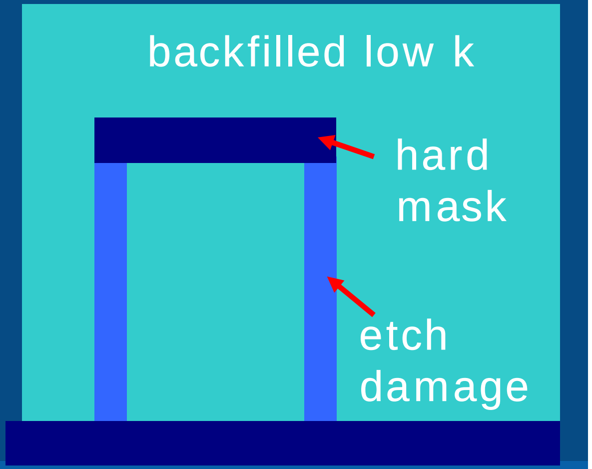

backfilled low k

hard mask

etch damage

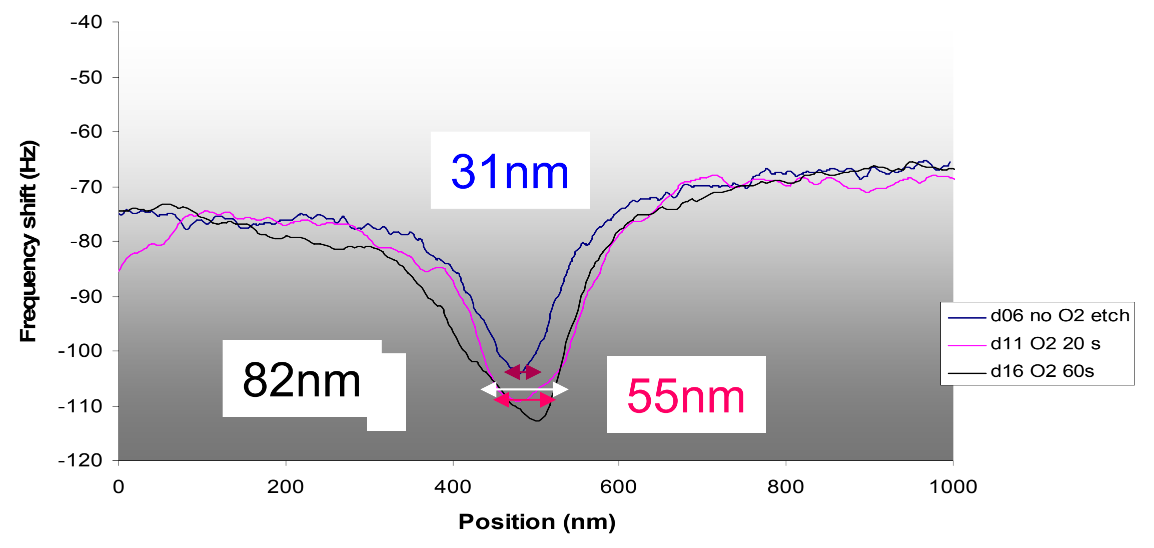

31nm

82nm

55nm

Atom Probe (Physics)

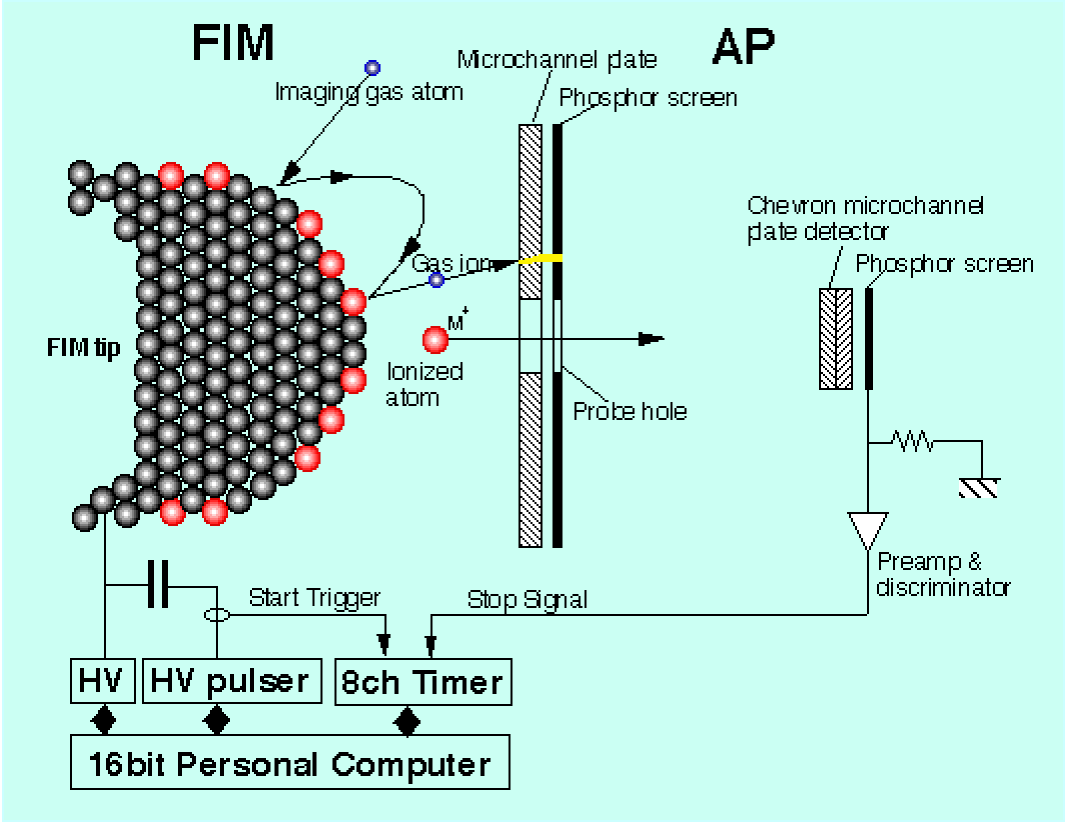

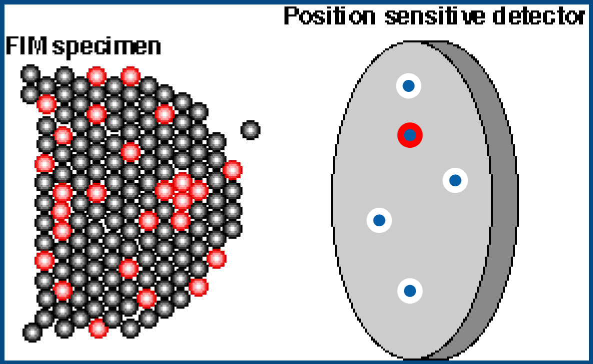

3D Atomic Mapping

- transist time ~ mass
- (x,y) detector ~ position
- time evolution ~ depth

- Can provide 3D chemical imaging with atomic resolution
- Technique is slow and requires needle-like sample prep

Atom Probe (Example)

[3] Perea

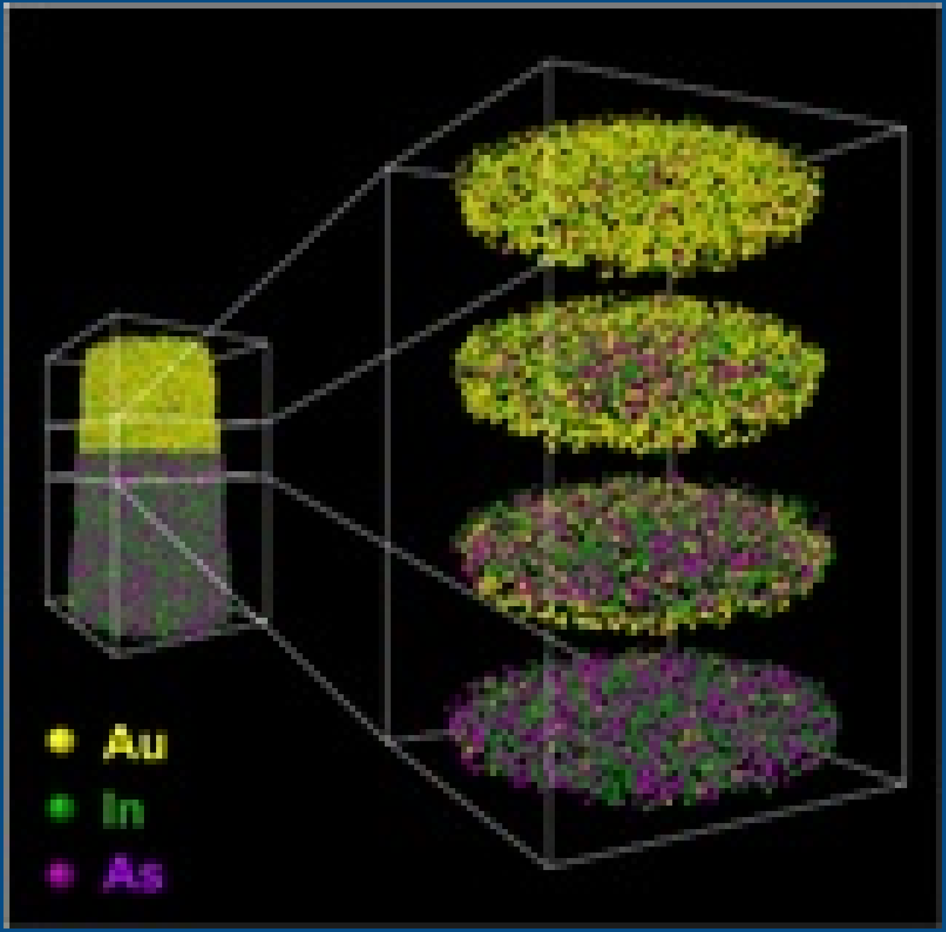

InAs Nanowire Tip (grown with Au catalyst by vapor-liquid-solid method)

- 14 nm diameter wire
- 23 nm tall
- Dots are atoms
- Exploded view at right

Coventional TEM (Physics)

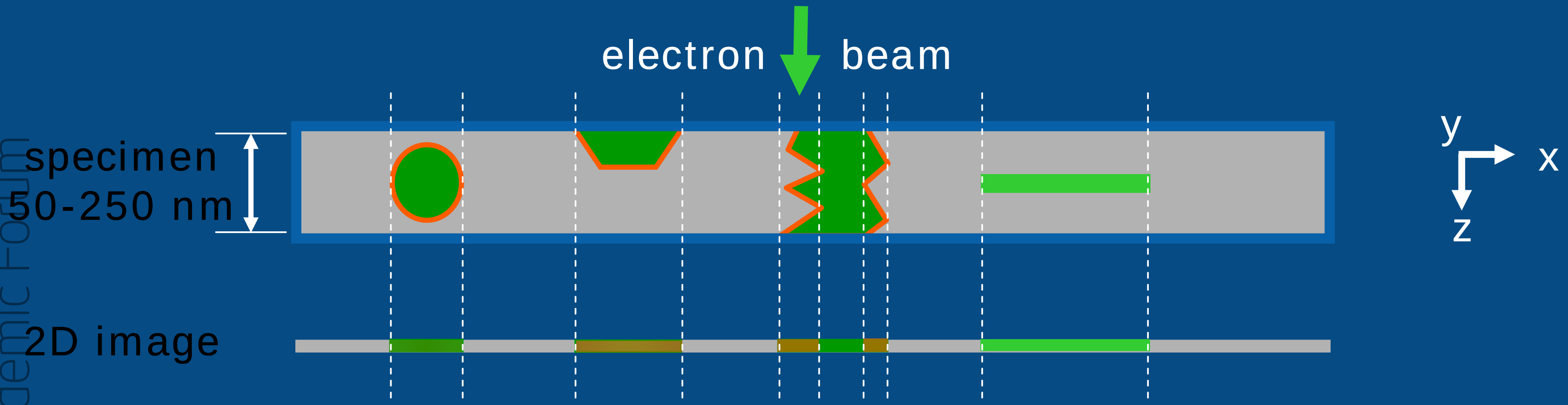

- nano-structure are smaller than the TEM specimen thickness
- interfaces are not edge-on

- 2D-projection gives rise to blurring/overlap which hampers the interpretation and metrology

TEM Tomography (Physics)

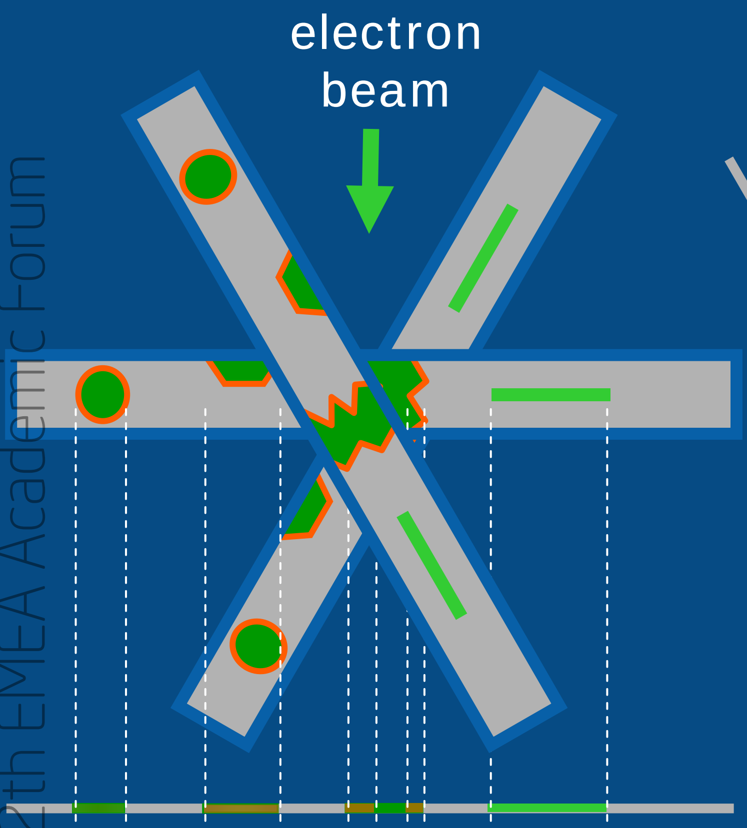

specimen 250 nm
tilted +/-75º, 1º increment
151 2D image

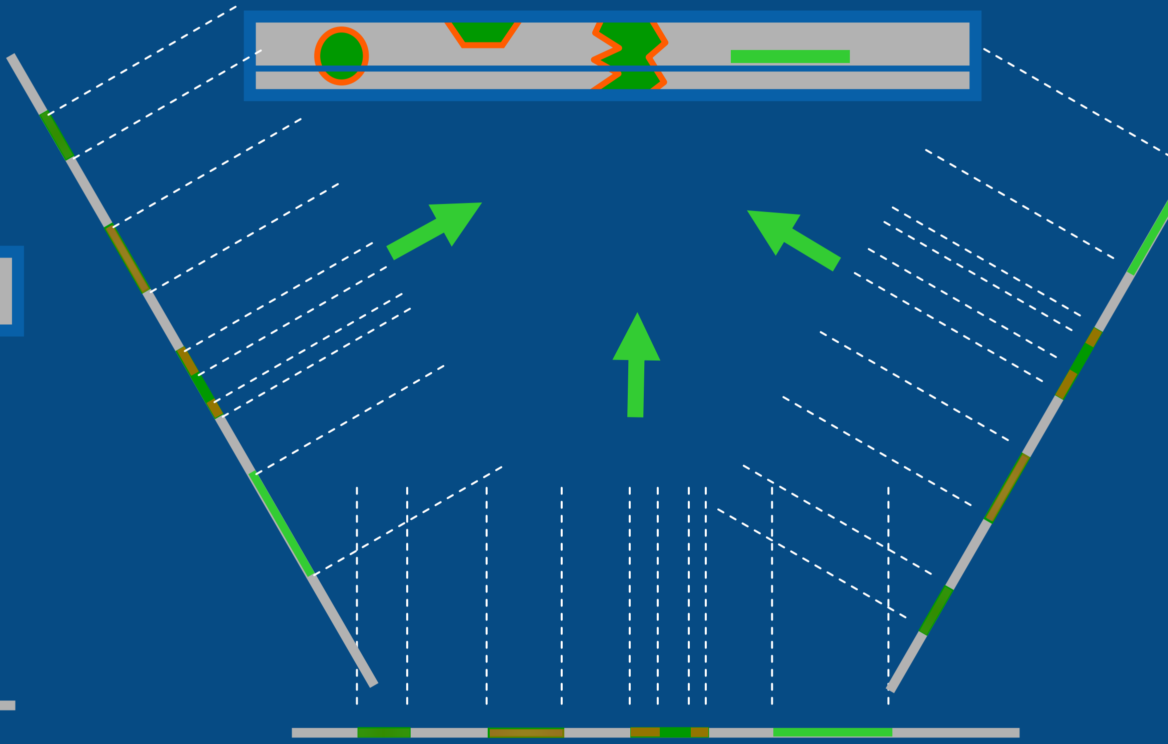

backprojection 151 2D images
reconstruction of the
3D volume
slices through the volume

TEM Tomography (Example)

[4] Bender

FINFET:

Fin and gate < 20 nm

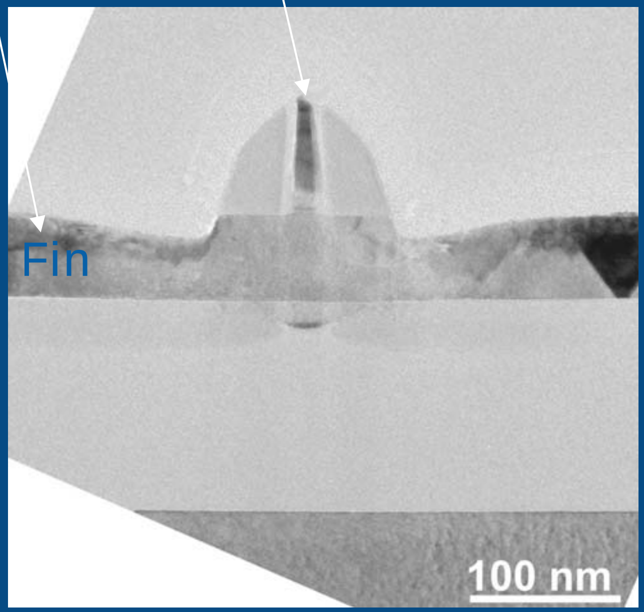

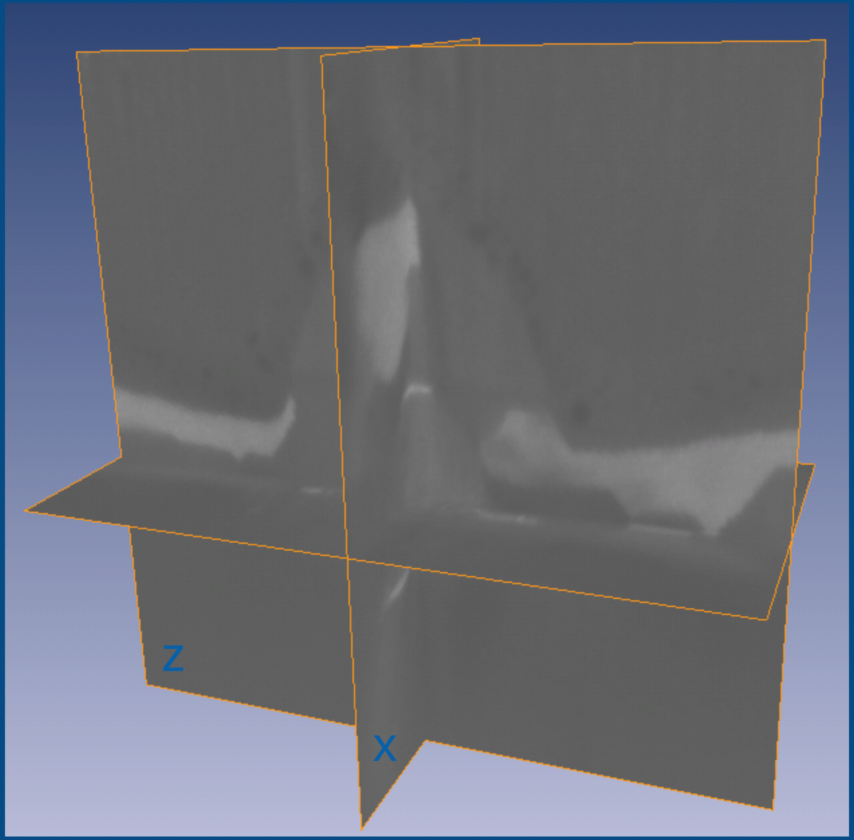

TEM Tomography (Example)^{4} Bender

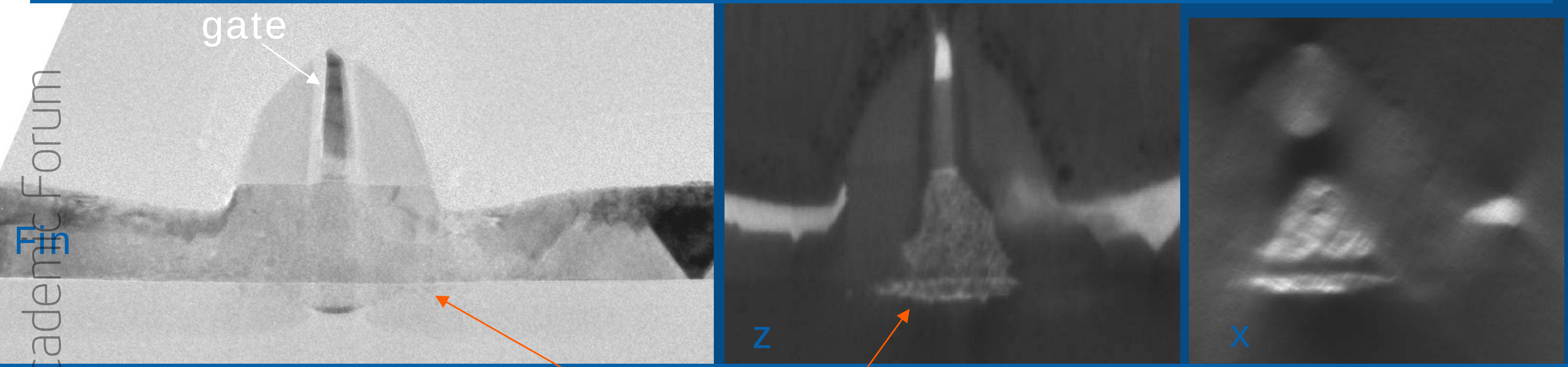
TEM

tomography slices

HfO_2 – trapezoid invisible on TEM image

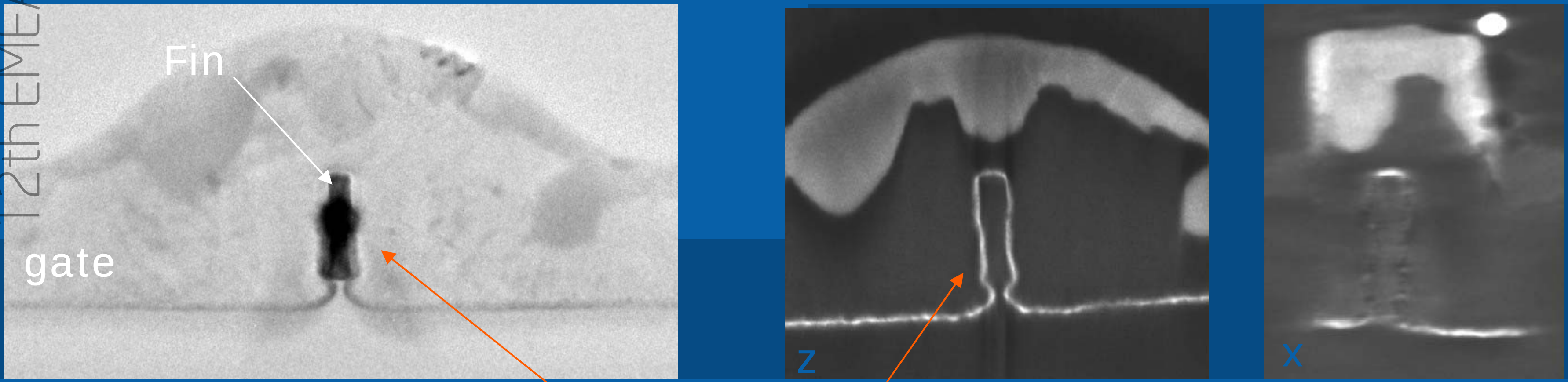

HfO_2 layer thickness on FIN-sidewall: unclear on TEM image

100 nm

Electron Spin Resonance (Physics)

- **ESR can probe unpaired electron trap levels in dielectric materials as a function of material, process and electrical processing.**

Zeeman splitting:
$\Delta E = g\mu_B B$

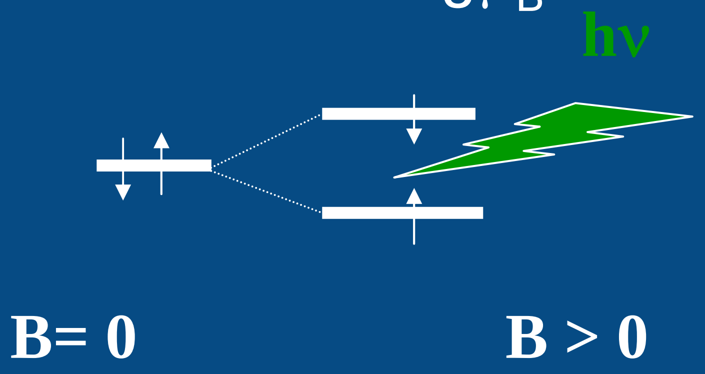

- Each defect has it's unique ESR signature of energy and electronic g-factor

Electron Spin Resonance (Example)

ESR spectra for different low k materials and treatments:

[5] Shamuilia

Name	Nature
P_{b0}	Interfacial dangling bond
P_{b1}	Interfacial dangling bond
E'_{γ}	Hole trapped on O vacancy
EX	Delocalized O hole
Si:P	P dopant in Si

- Different defects are observed in different pristine dielectrics

- Etch damage induces large changes in defect densities

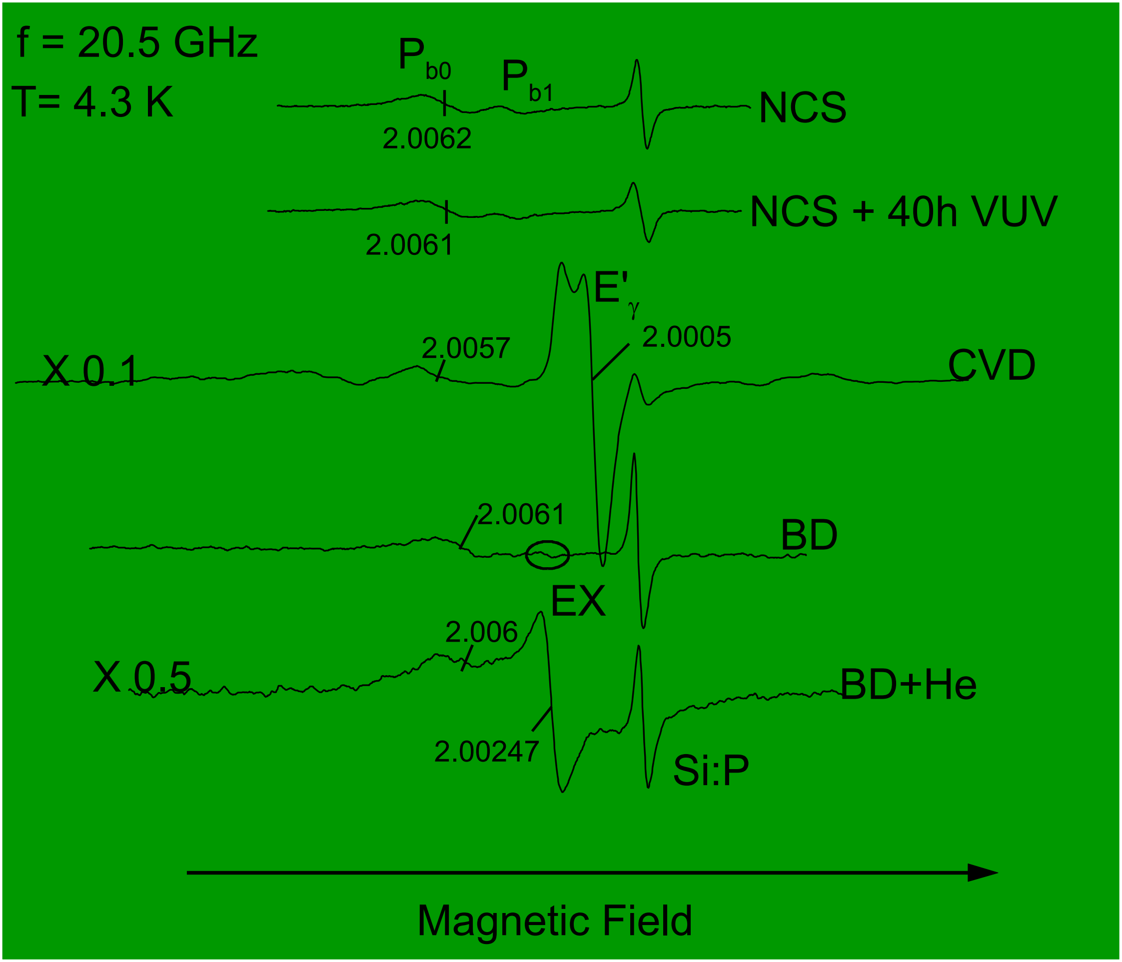

Interface Characterization

- **Interfaces**
  - Sidewall damage/etch residues
  - Thin barriers
  - Sidewall scattering

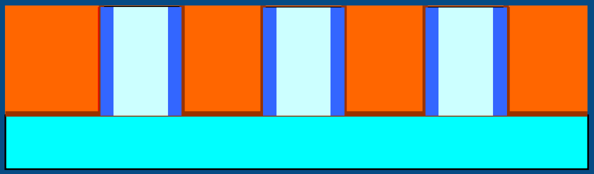

Interface Characterization Gaps

1) Sidewall roughness in sub 50 nm trenches

2) Transport measurements differentiating SW scattering from grain boundary scattering

Low k & Cu Structure Characterization

- **Low k & Cu Structure**
  - Porosity and Sealing
  - Bonding Structure
  - Barrier and Cu texture/grain size

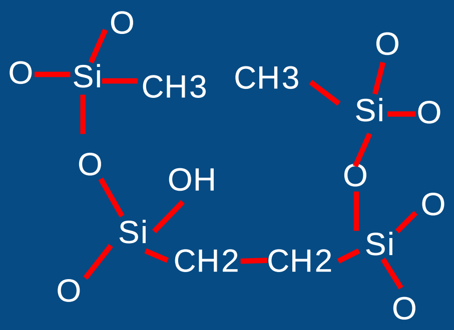

Novel Characterization Techniques

Ellipsometric Porosimetry
Extended X-ray Absorption Spectroscopy
Near Edge X-ray Absorption Spectroscopy
Nuclear Magnetic Resonance

Ellipsometric Porosimetry (Physics)

In EP, ε is measured in the range of visible light, when absorption of low-k films is negligible and $\varepsilon = n^2$.

Dense prototype:

$$B_1 = \frac{n_r^2 - 1}{n_r^2 + 2} = \frac{n_2^2 - 1}{n_2^2 + 2}$$

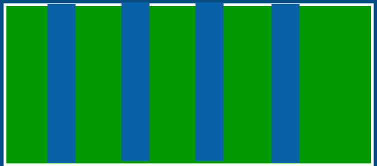

Empty pores:

$$B_2 = \frac{n_r^2 - 1}{n_r^2 + 2} = V\frac{n_1^2 - 1}{n_1^2 + 2} + (1 - V)\frac{n_2^2 - 1}{n_2^2 + 2}$$

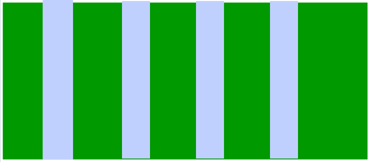

Liquid in pores:

$$B_3 = \frac{n_r^2 - 1}{n_r^2 + 2} = V\frac{n_{ads}^2 - 1}{n_{ads}^2 + 2} + (1 - V)\frac{n_2^2 - 1}{n_2^2 + 2}$$

1. Dense prototype: The skeleton refractive index $\boldsymbol{n_2}$ defines the measured refractive index $\boldsymbol{n_r}$ and Volume Polarisability $\boldsymbol{B_1}$.
2. Empty pores: $\boldsymbol{n_1}$=1 and Volume Polarisability ($\boldsymbol{B_2}$) depends on skeleton refractive index and porosity.
3. Pore filled by liquid: Volume Polarisability ($\boldsymbol{B_3}$) depends on skeleton refractive index, refractive index of the condensed liquid and porosity.

Comparison of (2) and (3) gives information about amount of open and closed pores.

Ellipsometric Porosimetry

[6] Baklanov

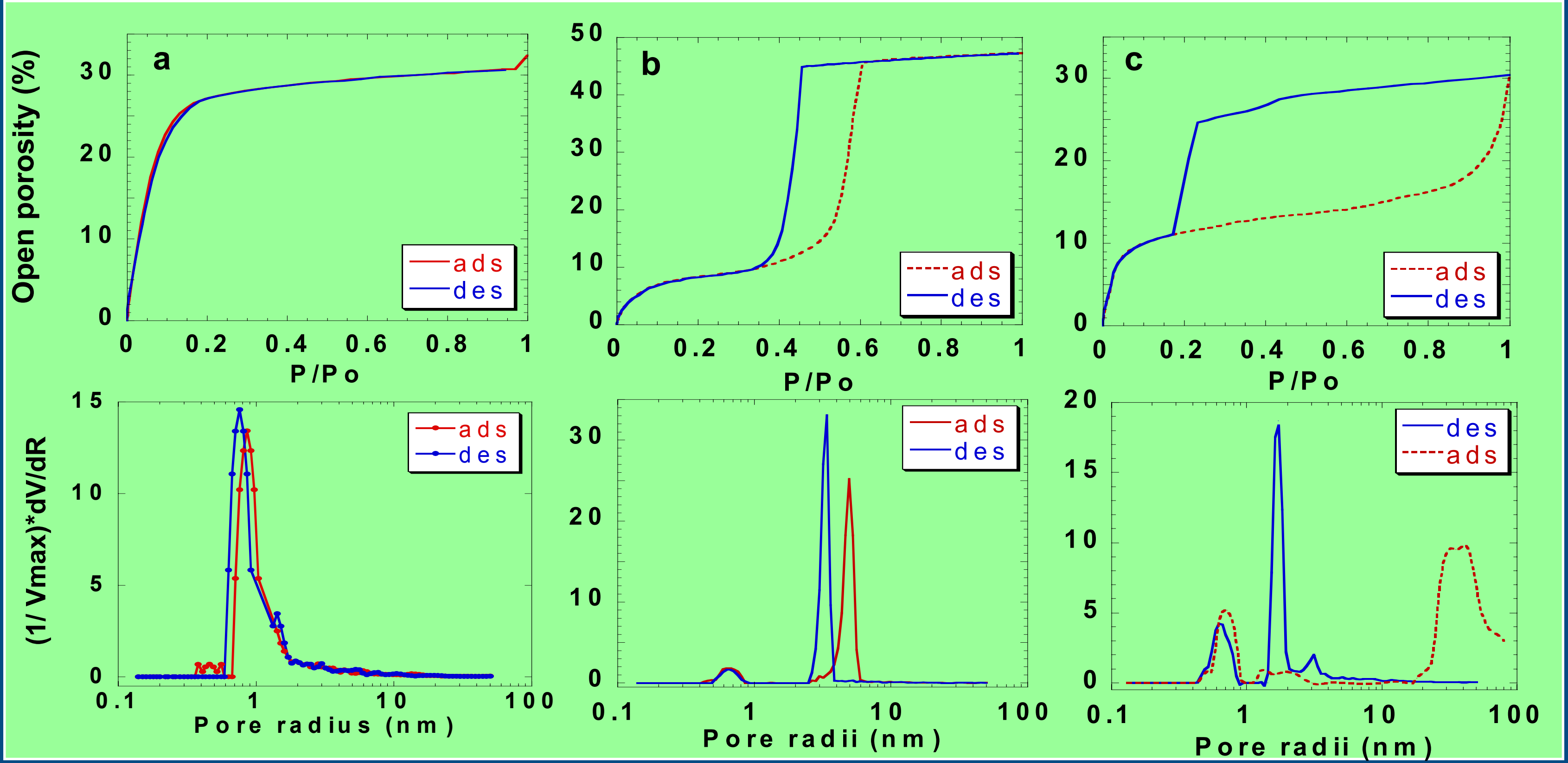

toluene

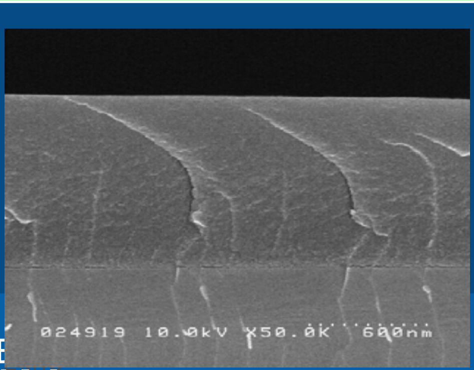

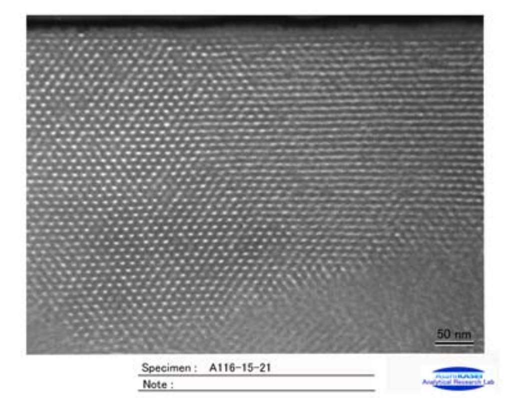

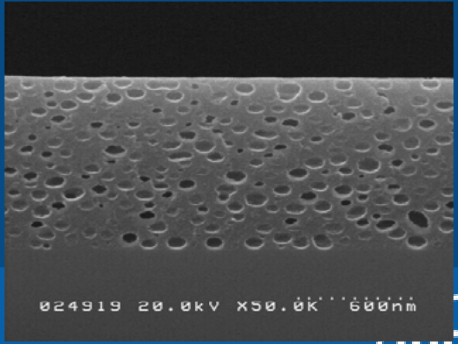

Ellipsometric Porosimetry (Example)

6 Baklanov

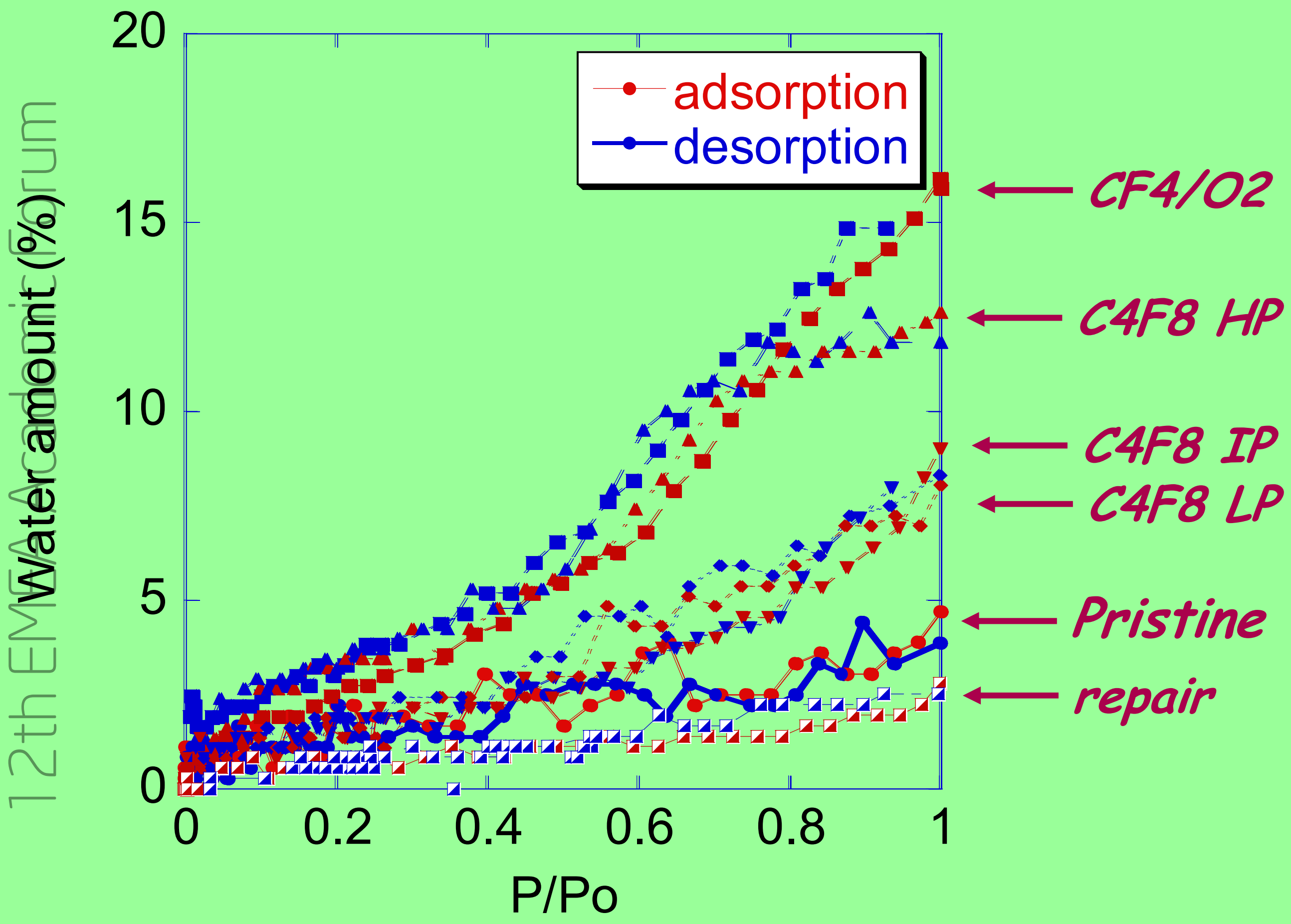

Etch chemistry vs water absporption

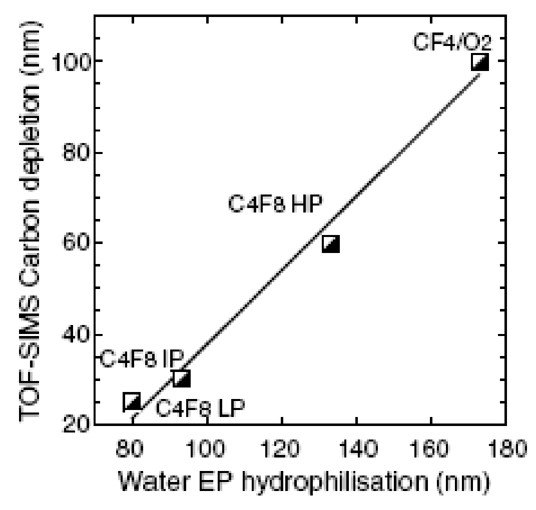

Good correlation between internal hydrophilicity and TOF-SIMS carbon depletion

Extended X-ray Absorption Spectroscopy (Physics)

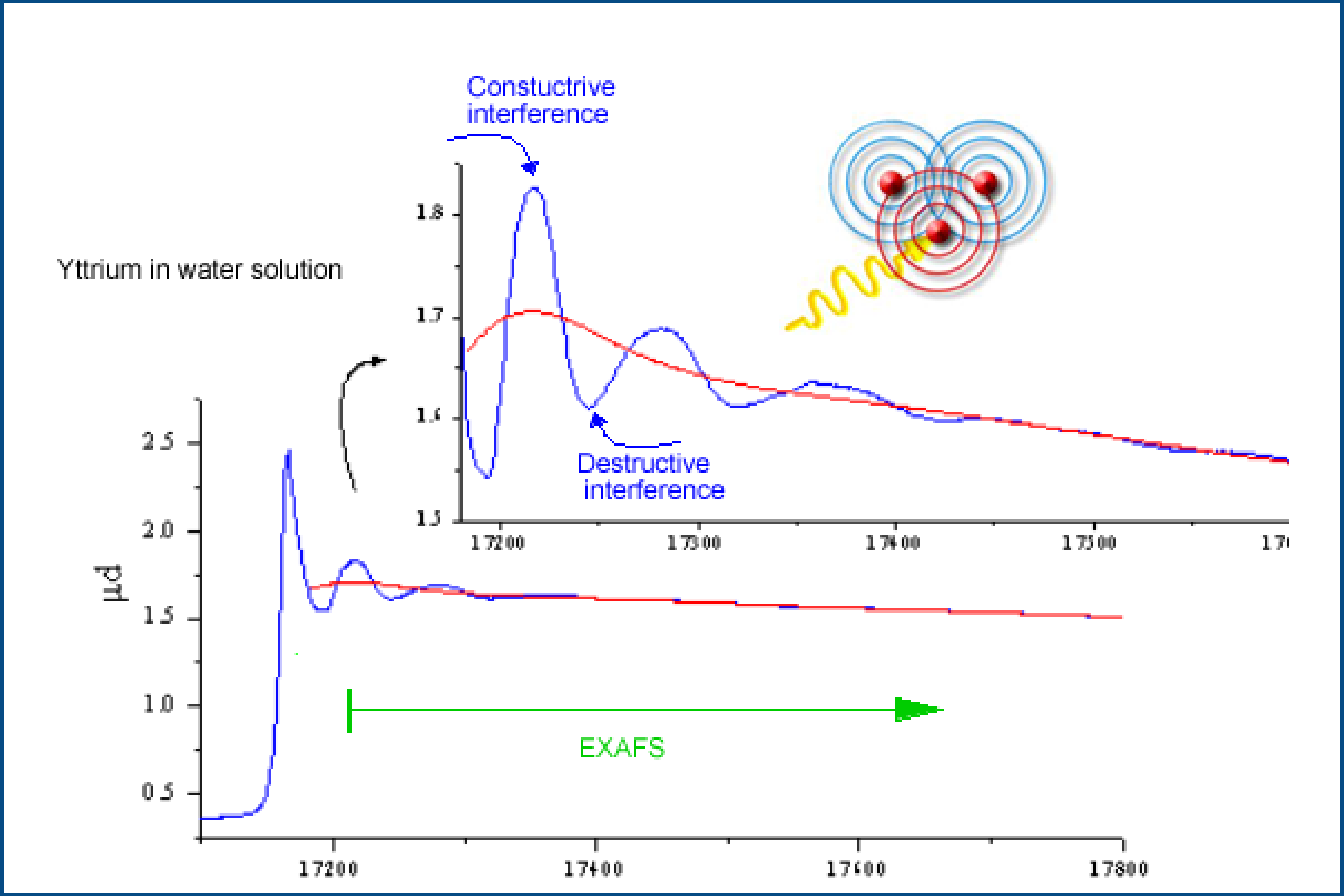

Extended X-ray Absorption Spectroscopy (Physics)

Wavevector k:

$k = 2\pi / \lambda_{dB}$ ← photoelectron de Broglie wavelength

$$k = \sqrt{\frac{2m\,(E-E_{edge})}{\hbar}}$$

Absorption χ:

$\chi(k) = (\mu-\mu_0)/\Delta\mu_0$

$$\chi_i(k) = \sum_j \frac{N_j B_j(k)}{r_j^2} e^{-2r_j/\lambda(k)} e^{-2k^2\sigma_j^2} \sin\left(2kr_j + \delta_j(k)\right)$$

Extended X-ray Absorption Spectroscopy (Example)

[7] Ablett

5 nm TaN / 20 nm Ta Barrier

2 scans, 2hours

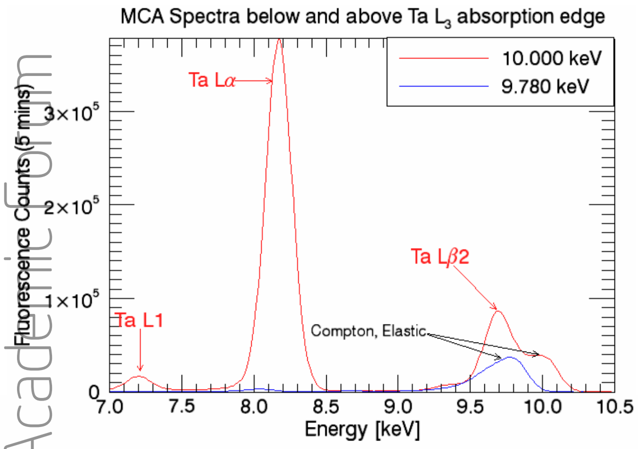

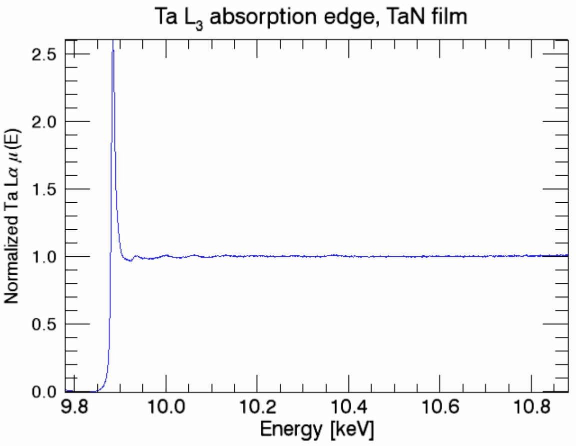

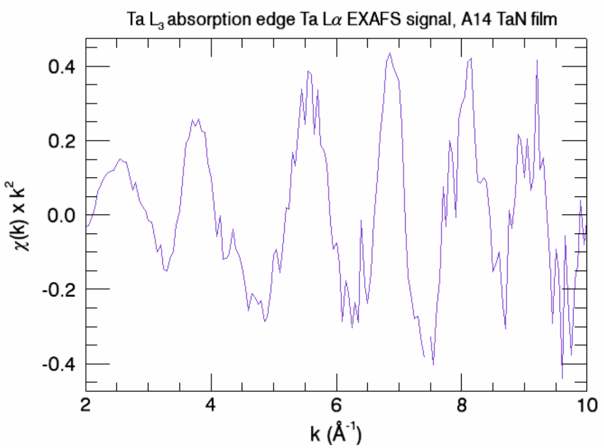

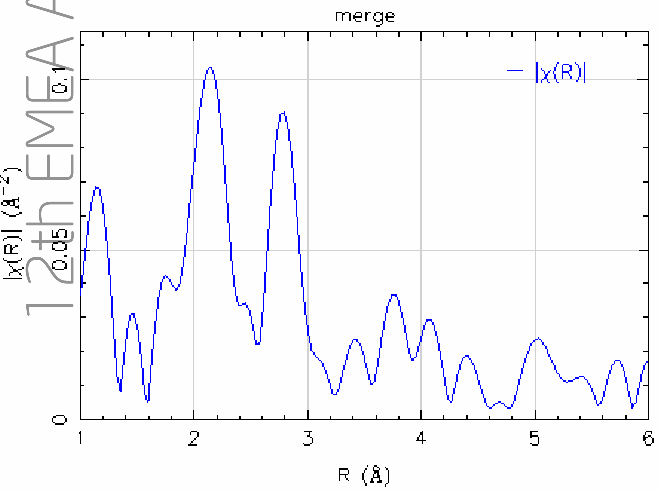

- Can probe local bonding (nn)
- Can see through Cu and passivation with x-rays
- Seems to have both α and β Ta

Near Edge X-ray Absorption Spectroscopy (Physics)

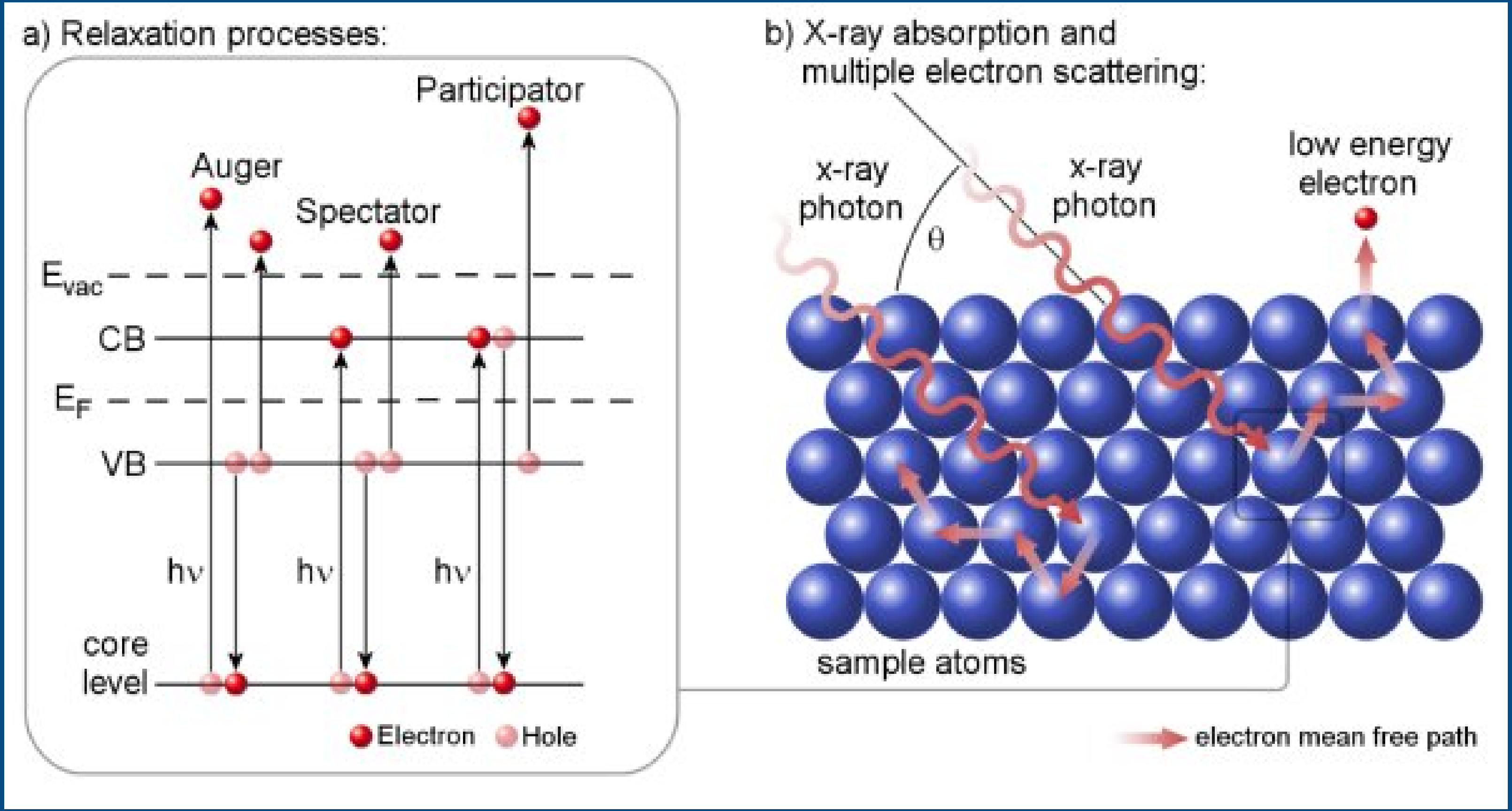

NEXAFS is sensitive to:

- unfilled molecular orbitals
- bond angles
- degree of local ordering

Near Edge X-ray Absorption Spectroscopy (Physics)

^{8} Iacopi

C K edges

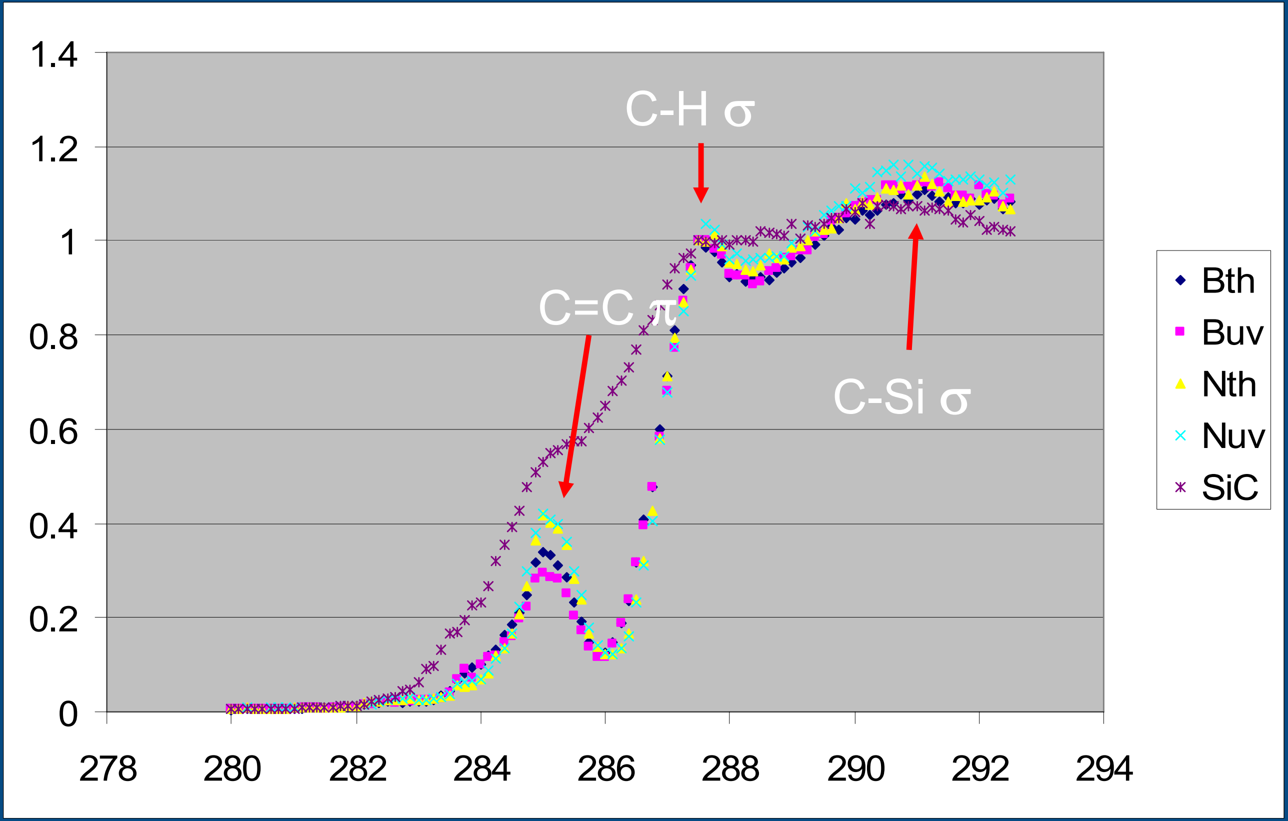

- C local environment is very similar for all low k materials
- SiC has more C π bonding

Near Edge X-ray Absorption Spectroscopy (Example)

[8] Iacopi

Si K edge

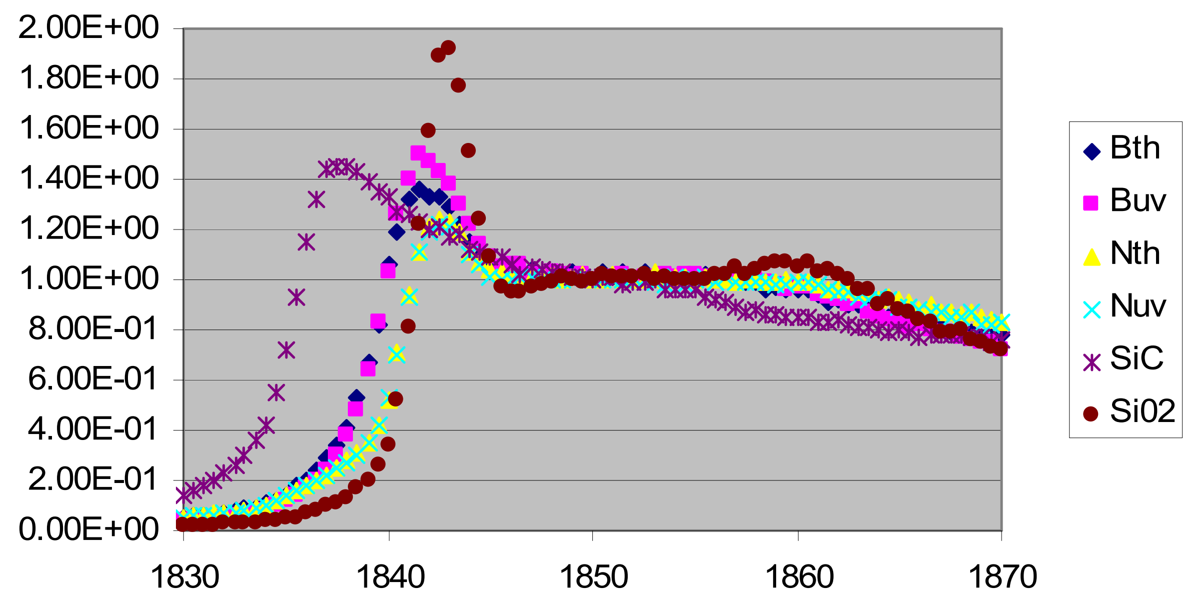

- Thresholds of SiC < BDI <NCS <SiO2 (% SiC vs SiO bond)
- UV sharpens BDI peak, increased ordering
- UV has no impact on NCS, high porosity reduces resonance

Nuclear Magnetic Resonance (Physics)

Resonant RF absorption for:

$$\nu = \gamma B_0 (1-\sigma)/2\pi$$

$$\delta_{ppm} = (\nu_s - \nu_r) \times 10^6/\nu_r$$

γ gyromatic ratio
σ shielding factor
δ_{ppm} chemical shift

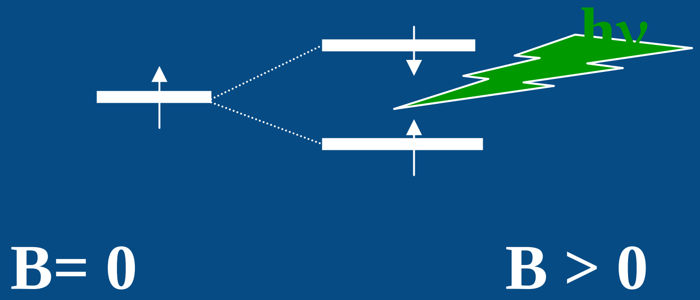

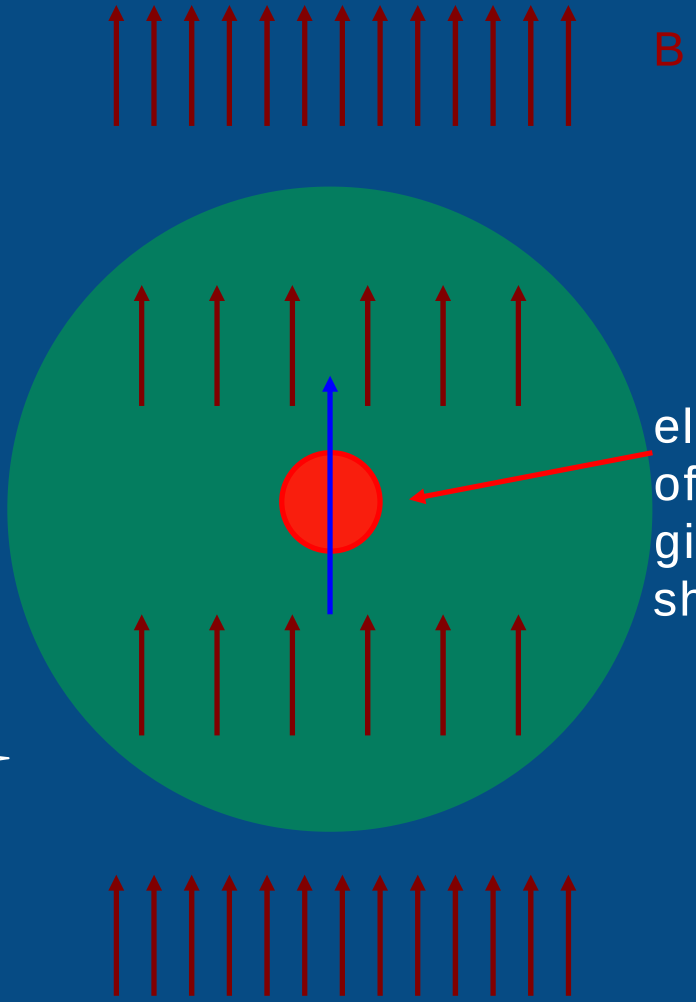

electron shielding of B at nucleus gives chemical shift

Nuclear Magnetic Resonance (Physics)

[9] Mabboux

M

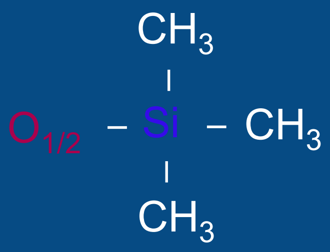

$$\begin{array}{ccccc} & & CH_3 & & \\ & & | & & \\ O_{1/2} & - & Si & - & CH_3 \\ & & | & & \\ & & CH_3 & & \end{array}$$

D

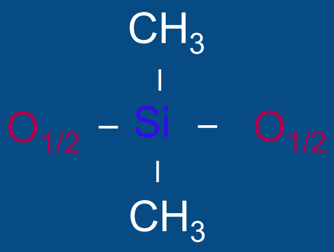

$$\begin{array}{ccccc} & & CH_3 & & \\ & & | & & \\ O_{1/2} & - & Si & - & O_{1/2} \\ & & | & & \\ & & CH_3 & & \end{array}$$

T

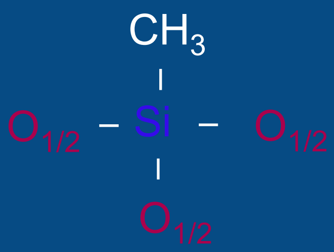

$$\begin{array}{ccccc} & & CH_3 & & \\ & & | & & \\ O_{1/2} & - & Si & - & O_{1/2} \\ & & | & & \\ & & O_{1/2} & & \end{array}$$

Q

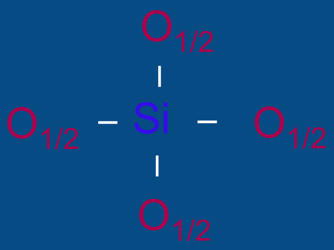

$$\begin{array}{ccccc} & & O_{1/2} & & \\ & & | & & \\ O_{1/2} & - & Si & - & O_{1/2} \\ & & | & & \\ & & O_{1/2} & & \end{array}$$

D_{OH}

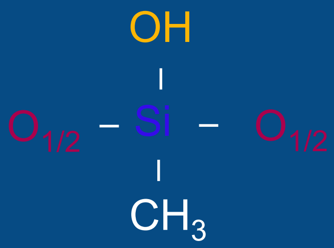

$$\begin{array}{ccccc} & & OH & & \\ & & | & & \\ O_{1/2} & - & Si & - & O_{1/2} \\ & & | & & \\ & & CH_3 & & \end{array}$$

T_{OH}

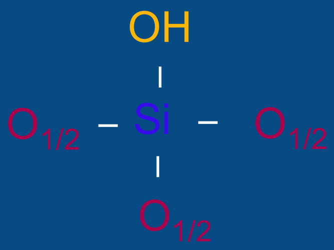

$$\begin{array}{ccccc} & & OH & & \\ & & | & & \\ O_{1/2} & - & Si & - & O_{1/2} \\ & & | & & \\ & & O_{1/2} & & \end{array}$$

Lowest crosslinked → Highest crosslinked

D_{OMe}

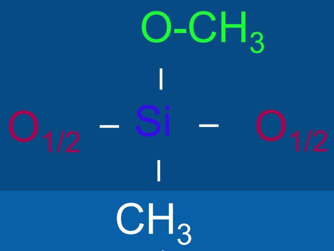

$$\begin{array}{ccccc} & & O\text{-}CH_3 & & \\ & & | & & \\ O_{1/2} & - & Si & - & O_{1/2} \\ & & | & & \\ & & CH_3 & & \end{array}$$

Nuclear Magnetic Resonance (Example)

[10] Abell

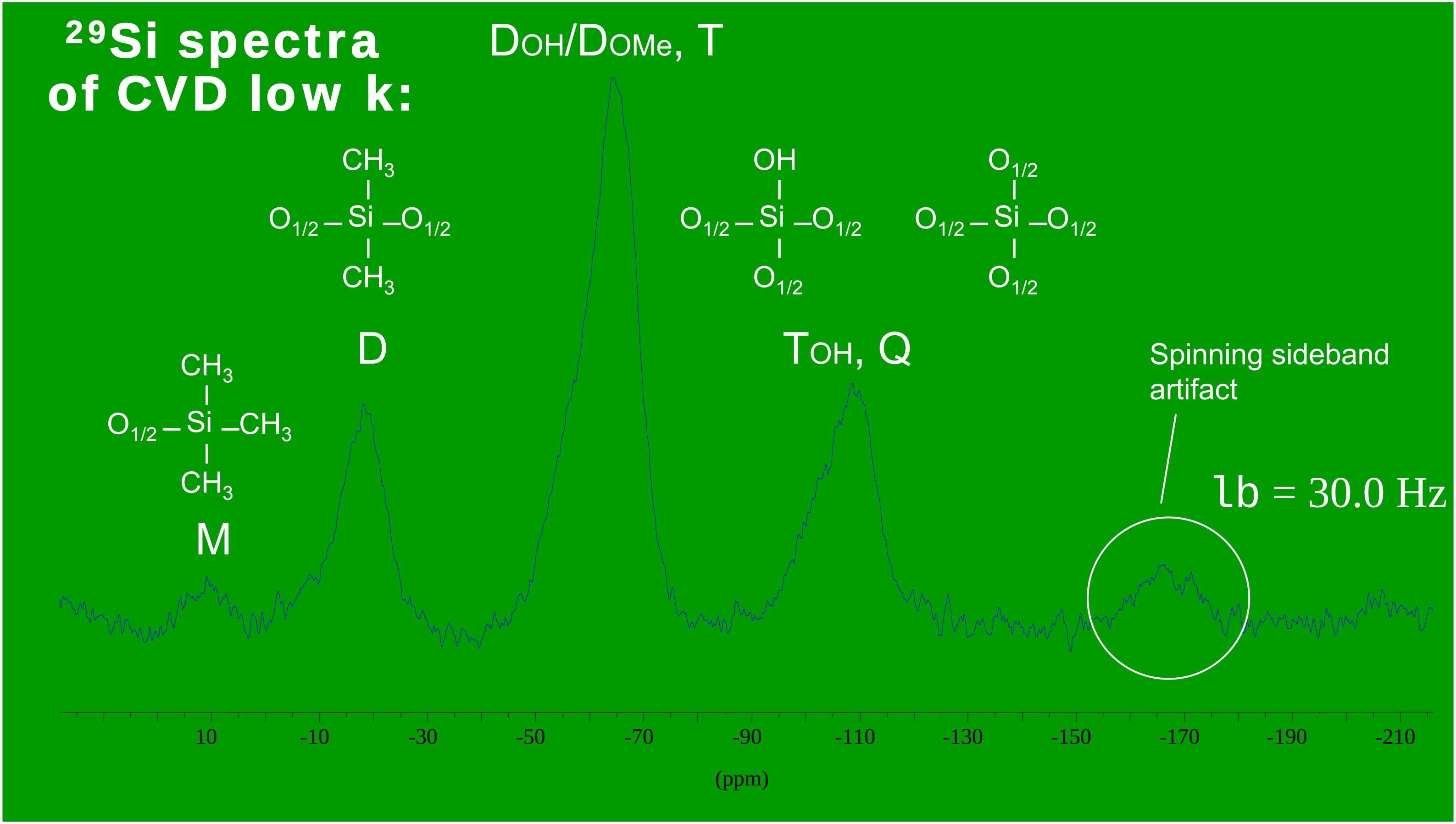

^{29}Si spectra of CVD low k:

- Peaks are still broad compared to single lines for liquid NMR
- D_{OH}/D_{OMe} peak is left shoulder to main T peak
- T_{OH} peak is left shoulder to main Q peak

Low k & Cu Structure Characterization

- **Low k & Cu Structure**
  - Porosity and Sealing
  - Bonding Structure
  - Barrier and Cu texture/grain size

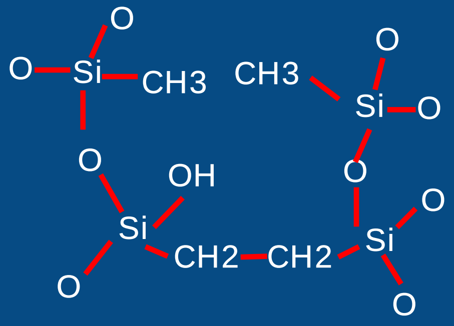

Low k & Cu Structure Characterization Gaps

1) Cu grain size and texture in sub-50 nm trenches

2) Trench sidewall damage / residues with sub 5 nm resolution

Mechanical Characterization

- **Mechanical Properties**
    - Young’s modulus, hardness
    - Adhesion
    - Fracture Dynamics

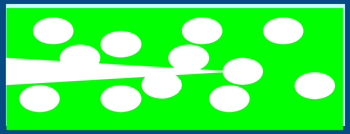

Novel Characterization Techniques

Cross-sectional Nanoindentation

Surface Acoustic Wave Spectroscopy

Brillouin Scattering

Cross-sectional Nanoindentation[11] Ocana (Physics)

Patterned films

- Quick turn monitor of adhesion in interconnect structures
- Good correlation with 4PB measurements in blanket

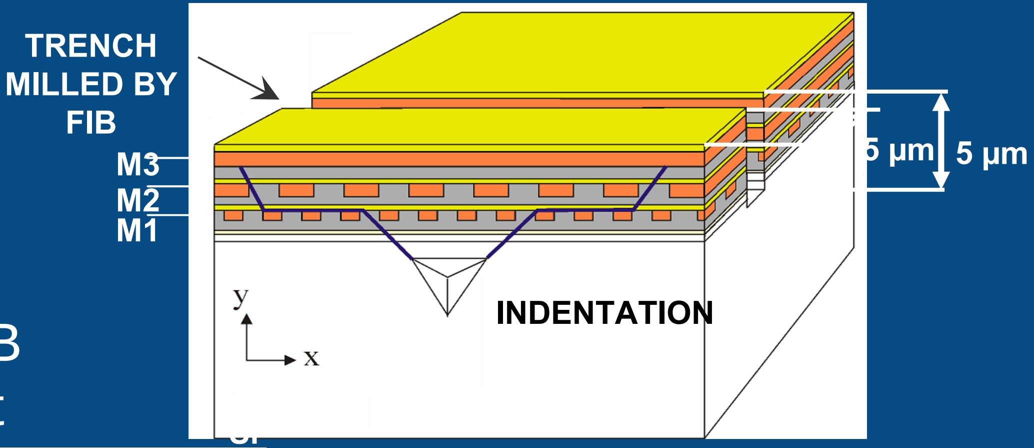

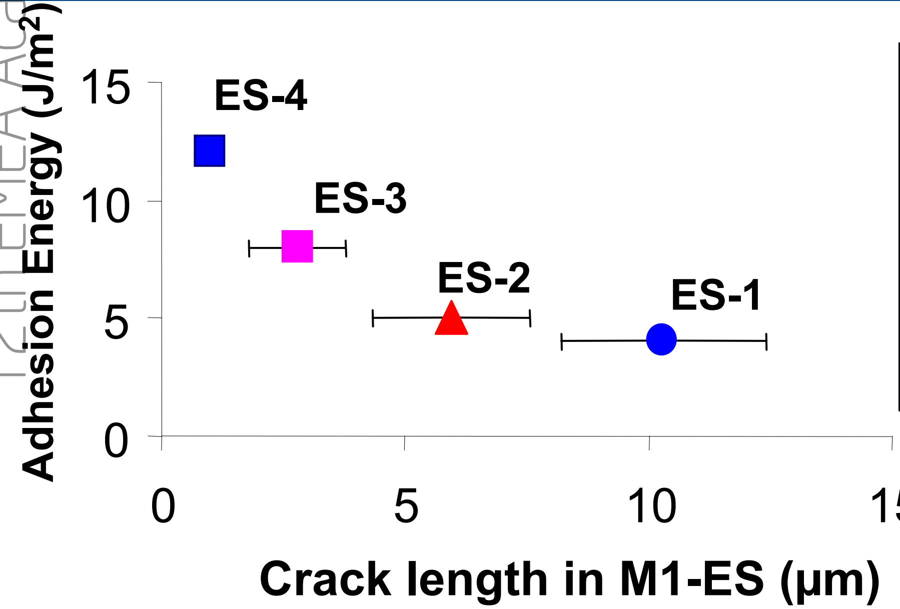

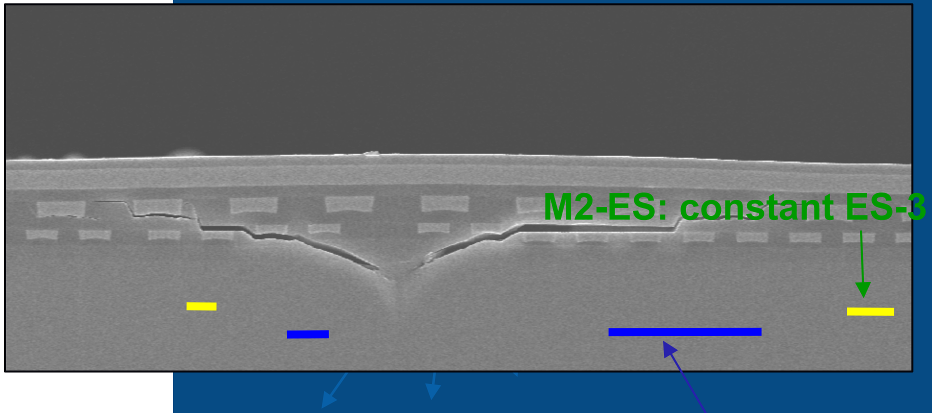

M1-ES: varying ES

Cross-sectional Nanoindentation (Example)

[11] Ocana

- Patterned films
  - FEM models with cohesive elements for crack growth studies in patterned structures
  - Fracture path depends upon relative values of cohesive and adhesive energies
  - Can also measure and model crack containment structures

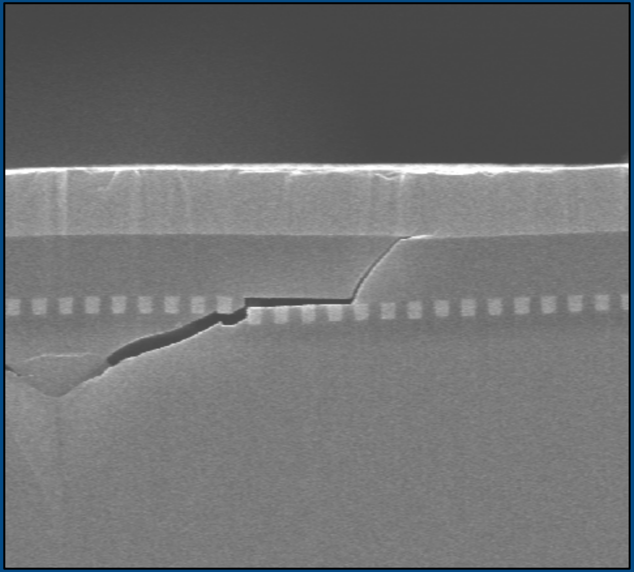

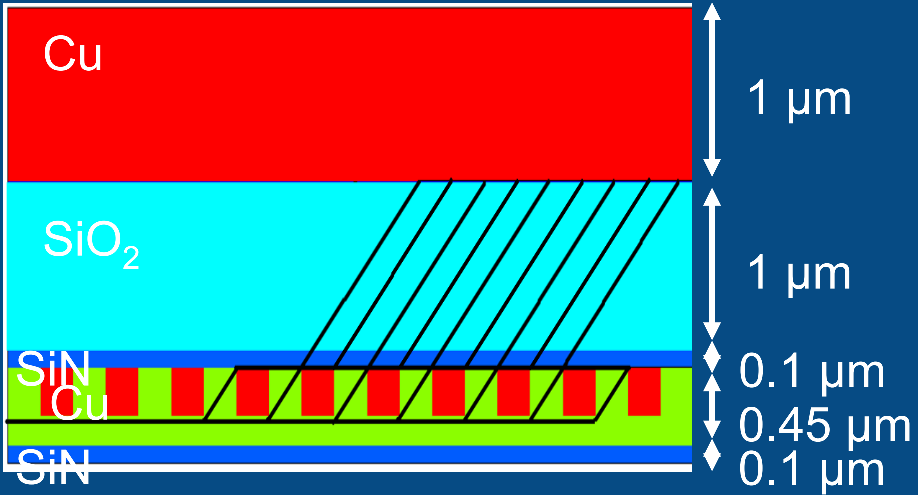

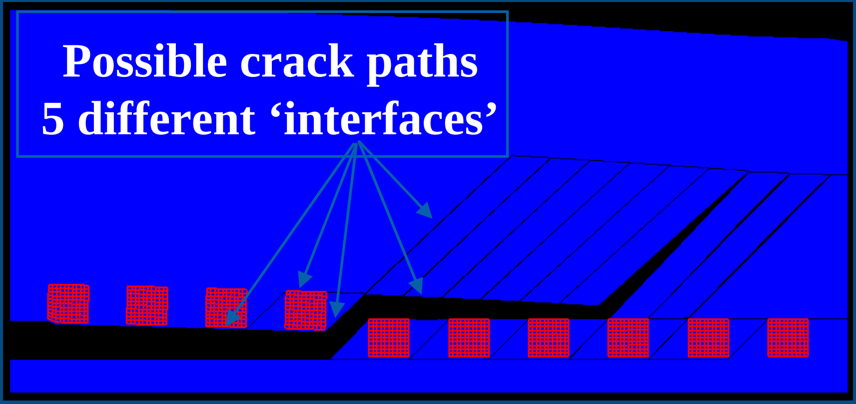

Possible crack paths
5 different 'interfaces'

Surface Acoustic Wave Spectroscopy (Physics)

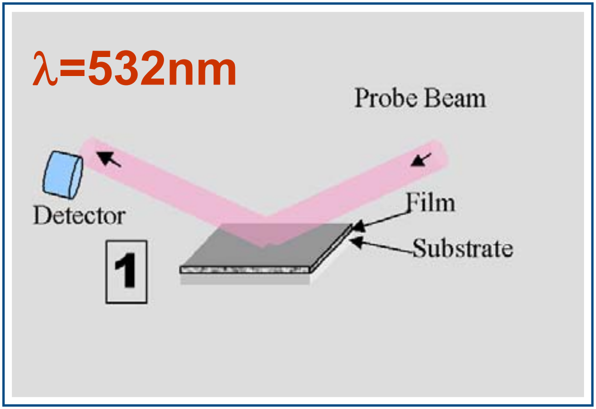

1. Dark signal before wave excitation.

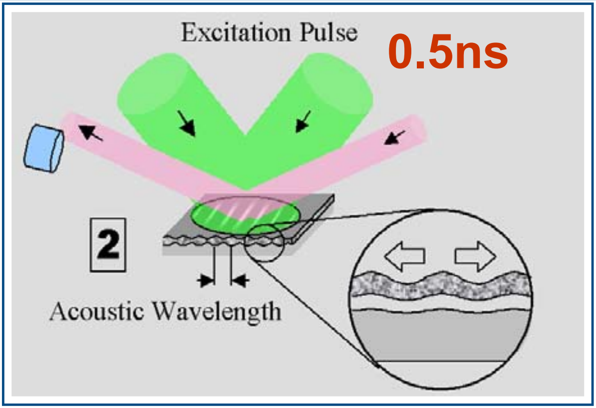

2. Wave excitation with striped pattern.

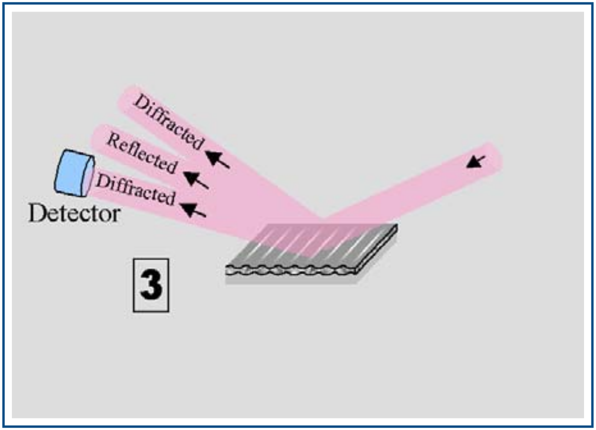

3. Wave motion and diffraction of probe beam to detector.

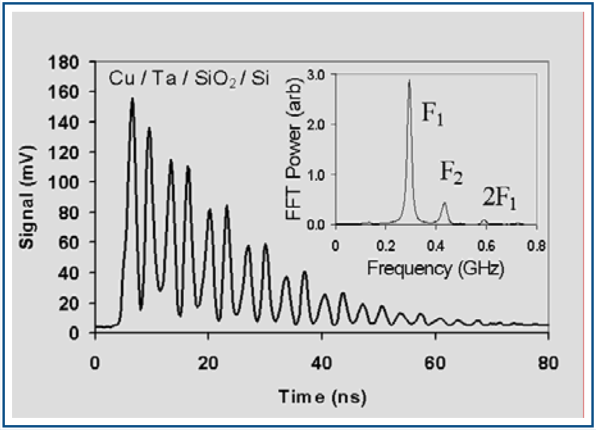

Waveform and frequency spectrum.

Surface Acoustic Wave Spectroscopy (Physics)

Elastic const.tensor

density

$$\rho \frac{\partial^2 u_j}{\partial t^2} - c_{ijkl} \frac{\partial^2 u_k}{\partial x_i \partial x_l} = 0$$

← Eq. motion volume element

$$Signal(t>0) \propto \Big[\overbrace{A_T \exp(-t/\tau)}^{\textit{Thermal Decay}} + \overbrace{A_1 \cdot G_1(t) \cdot \cos(2\pi F_1 t)}^{\textit{Acoustic Wave}} + \ldots\Big]^2$$

Acoustic Decay

Decay time

Frequency

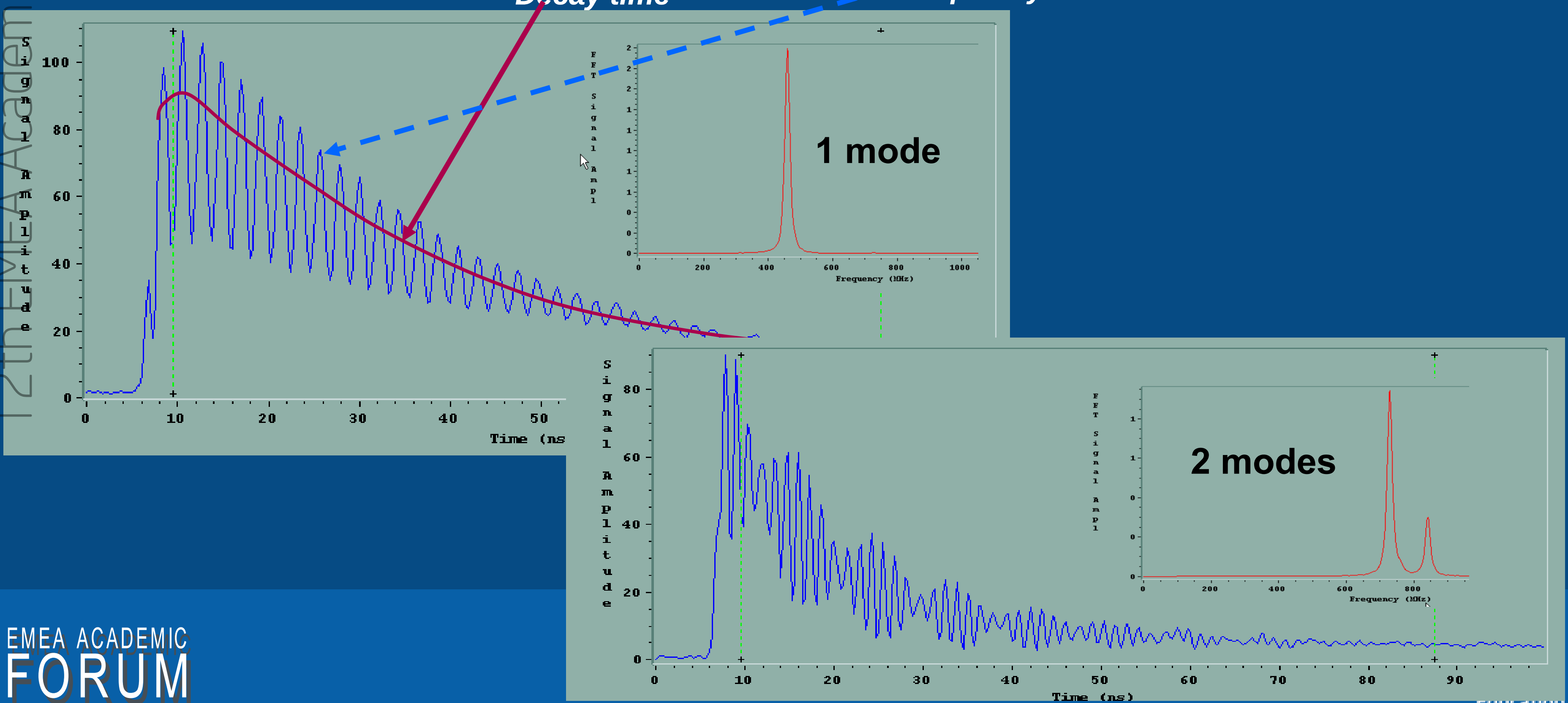

Surface Acoustics Wave Spectroscopy (Example)

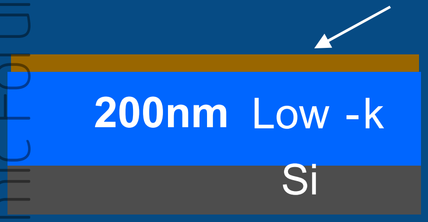

densified top layer

200nm Low -k

Si

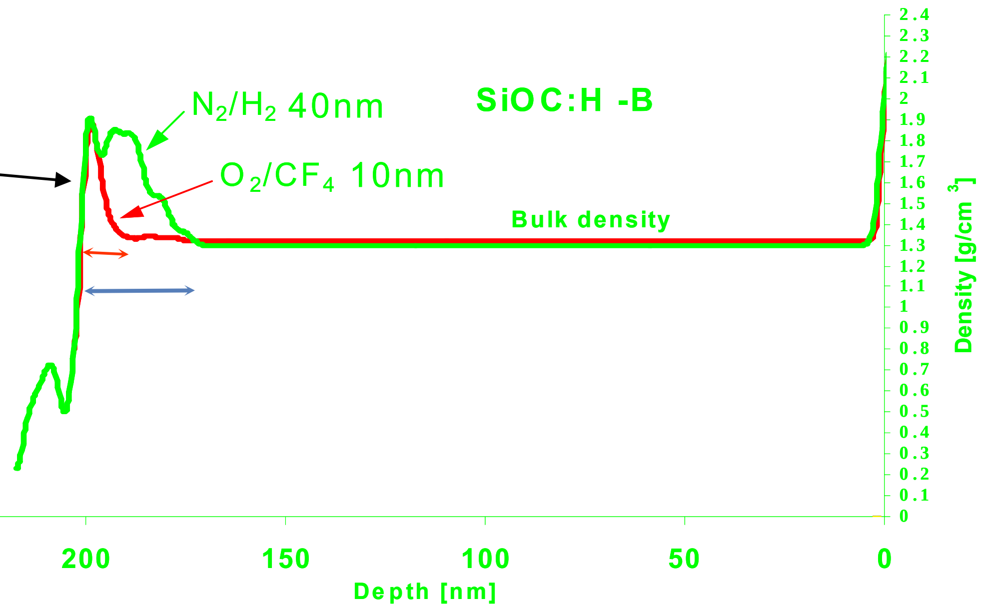

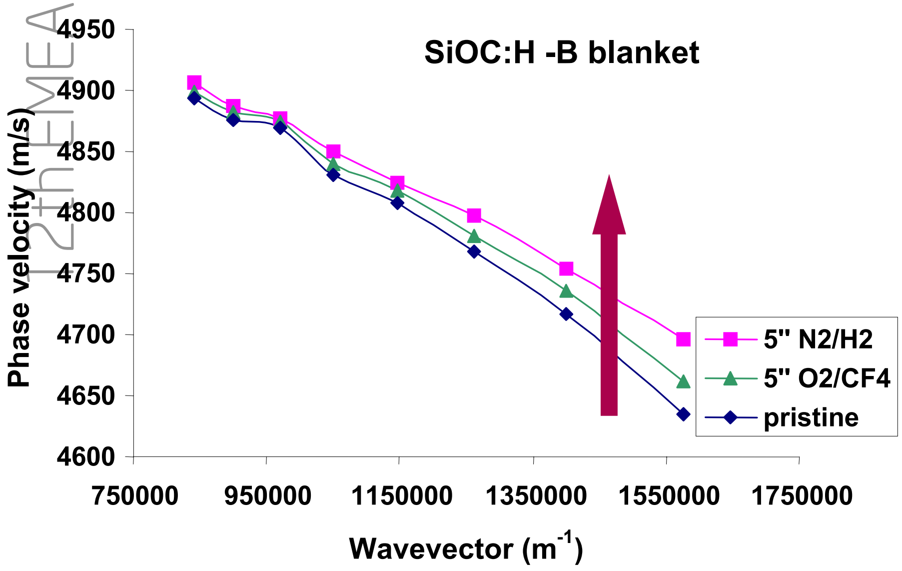

V increase for small λ: densification top layer!

Brillouin Scattering (Physics)

Inelastic scattering of photons by acoustic phonons, naturally present in the probed medium. The frequency range of phonons is 1-100 GHz, depending on the material.

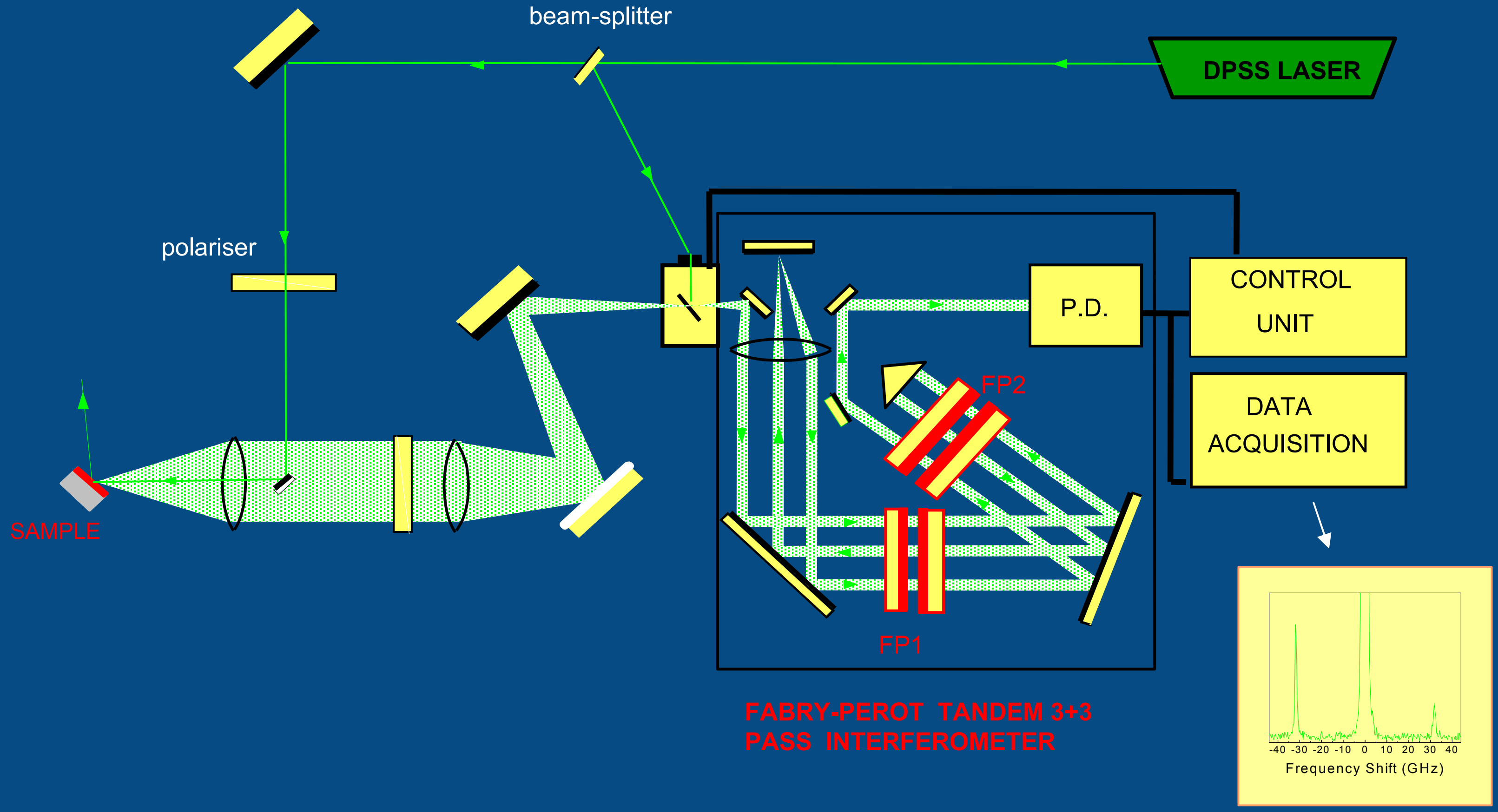

Brillouin Scattering (Physics)

For surface modes, only the parallel component of the wavevector is conserved in the scattering process.

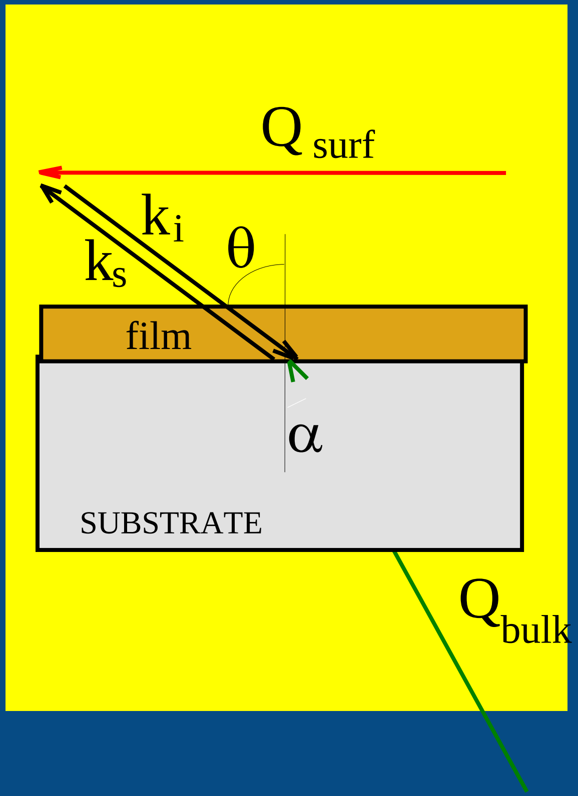

Incoming photons are scattered by two different mechnisms:

1. The rippling of the free surface induced by acoustic modes

2. The modulation of the dielectric constant inside the medium

For surface acoustic modes

$$Q_{surf} = 2k_i \sin(\theta) \rightarrow v = \frac{\pi f}{k \sin(\theta)}$$

For bulk acoustic modes

$$Q_{bulk} = 2nk_i \rightarrow v = \frac{\pi f}{n k}$$

Brillouin Scattering (Example)

[13] Carlotti

ZnO films on Si:

- Phonon dispersion
- Thin films
- Changes in phase velocity (frequency shift) depend differently on ρ and elastic constants fo different Rayleigh modes

Phonon Dispersion

Thin Films ~ 20 nm

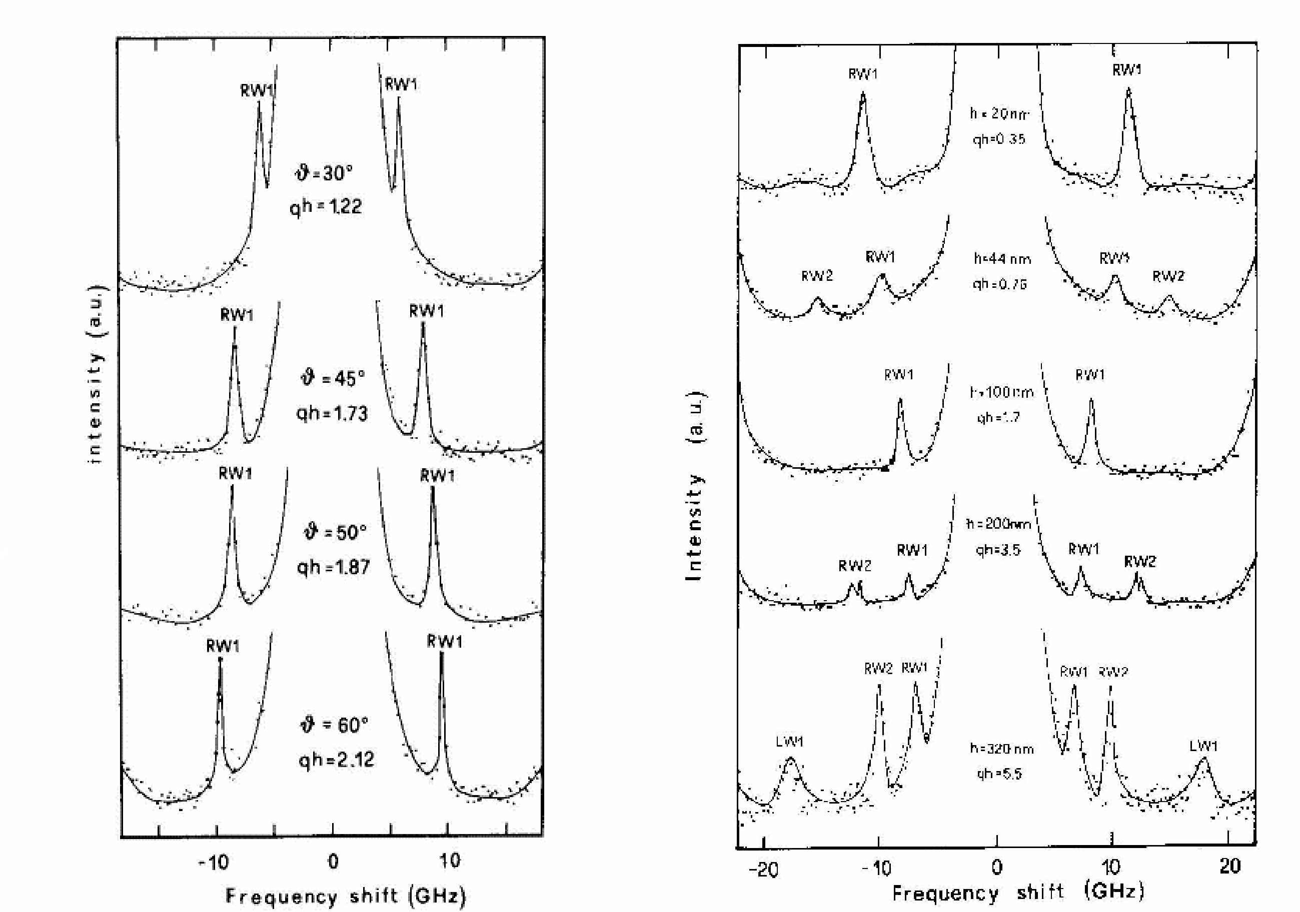

Mechanical Characterization

- **Mechanical Properties**
  - Young’s modulus, hardness
  - Adhesion
  - Fracture Dynamics

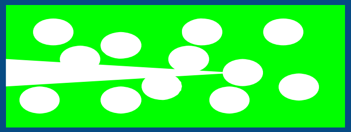

Mechanical Characterization Gaps

1) Pre-existing sub-critical cracks

2) Mechanical properties of patterned dielectric structures

Characterization Conclusions I

Interfaces:

- Several promising 3D imaging techniques with atomic resolution (TEM tomography and atom probe) are being developed but require challenging sample preparations.

- Need for sidewall roughness and scattering mechanism metrology.

Low k and Cu Structure:

- Ellipsometric porosimetry offers potential for in line probing of pore fraction, pore size and hydrophobicity.

- Several techniques show promise for probing the structure of low k and metal bonding at dedicated facilities (EXAFS, NEXAFS and NMR).

- Need for small grain Cu and high resolution sidewall damage metrologies

Characterization Conclusions II

Mechanical Properties:

- Two in line optical techniques show great promise for in line metrology of thin dielectric mechanical properties (SAWS and Brillouin scattering)

- Cross sectional nanoidentation provides an interesting option for probing mechanical properties and fracture dynamics in realistic structures.

- Need metrologies for sub-critical cracks and mechanical properties of patterned dielectrics.

References (I)

[1] Y. Travaly et. al, J. Appl. Phys. 97, 8, p 084316 (2005).

[2] T Gross, K. Soucy and E. Andideh, Proc. IEEE 2001 IITC, p 241 (2001).

[3] D. Perea et. al., Nano. Lett., 6 (2) p181 (2006).

[4] H. Bender et. al., Proc. 16th Intern. Microscopy Congress, Sapporo, p 1082 (2006).

[5] S. Shamuilia et. al., Appl. Phys. Lett. 89, p 202909 (2006)

[6] M. Baklanov, et.al., SiN and SiO2 Thin Insulating Films and Other Emerging Dielectrics VIII. ECS, 2005 p 179.

[7] J. Ablett, J. Woicik and Z. Tokei, Synchrotron Rad. Instrument. 9th Intern. Conf, 879, p 1557 (2007).

[8] F. Iacopi et. al., Acta Materialia 55 (4) p1407,(2007).

References (II)

[9] P. Mabboux and K. Gleason, J. Electrochem. Soc. 152 (1), pF7 (2005).

[10] T. Abell et. al., MRS Spring Meeting Proc. MRS vol. 863, (2005).

[11] I. Ocana et. al., MRS Spring Meeting Proc. MRS vol. 863, (2005).

[12] F. Iacopi et. al., Proc. IEEE 2005 and 2006 IITC.

[13] G. Carlotti, et. al., IEEE Trans. Ultrasonics, Ferroelectrics, 38, p56 (1991).